C-H Insertion and π-Complex Formation Reactions of $(\eta^5\text{-}C_5Me_5)(PMe_3)Ir$ with Ethylene: An Intra- and Intermolecular Isotope Effect Study

Page O. Stoutland and Robert G. Bergman*

Contribution from the Materials and Chemical Sciences Division, Lawrence Berkeley Laboratory, and the Department of Chemistry, University of California, Berkeley, California 94720.
Received November 24, 1987

Abstract: Thermolysis of the iridium cyclohexyl hydride $(\eta^5\text{-}Me_5C_5)(PMe_3)Ir(C_6H_{11})(H)$ at 130–160 °C in cyclohexane in the presence of ethylene results in formation of the vinyl hydride $(\eta^5\text{-}Me_5C_5)(PMe_3)Ir(HC{=}CH_2)(H)$ (**1**) and the π-complex $(\eta^5\text{-}Me_5C_5)(PMe_3)Ir(H_2C{=}CH_2)$ (**2**) in a ratio of 2:1. Thermolysis of **1** in cyclohexane or benzene above 180 °C results in quantitative conversion to **2**. Thermolysis of $(\eta^5\text{-}Me_5C_5)(PMe_3)Ir(C_6H_{11})(H)$ in the presence of ethylene-d_2 results in insertion into both the C–H and the C–D bonds and allows determination of an intramolecular isotope effect: $k_H/k_D = 1.18 \pm 0.03$. Competition experiments involving ethylene and ethylene-d_4 allow determination of an intermolecular isotope effect for insertion into a C–H(D) bond: $k_H/k_D = 1.49 \pm 0.08$. The intermolecular isotope effect for formation of **2** was found to be 0.82 ± 0.05. The different intra- and intermolecular isotope effects for C–H insertion require an intermediate different from the π-complex **2** on the reaction pathway leading to **1**. Possible structures for this species are discussed.

Alkenes are the group of organic molecules most frequently used in carbon–carbon and carbon–hydrogen bond-forming reactions mediated by organotransition-metal complexes. As a result, understanding the interaction of alkenes with transition-metal centers has been a central theme in organometallic chemistry almost since its inception.

Of key importance in the study of such reactions is an understanding of the primary interaction between the transition metal and the alkene; it is this that may control their selectivity. This is undoubtedly dependent on a variety of factors, including the following: whether the metal is present as a complex or as a surface, the steric environment and the electronic nature of the metal, and the type of hydrocarbon involved. In addition to this, one can envision several different ways in which a hydrocarbon bond is actually broken, resulting in the formation of new σ-bonds to the transition metal (C–H or C–C bond activation).

By far the most ubiquitous mode of metal–alkene interaction involves coordination of the metal center to the π-electrons of the alkene, leading to what is known as a π-complex or η^2-alkene complex. Such complexes have been known for over 150 years, and the metal–alkene interaction has been the subject of intense experimental and theoretical investigations. From these investigations a clear picture has emerged: electrons from an alkene π-orbital are donated to an empty d-orbital of the appropriate symmetry on the metal, and in some cases this is supplemented by the transfer of electron density from filled metal d-orbitals to the π*-orbital of the alkene. This can result in an exceptionally strong metal–alkene interaction.[1]

Many of the mechanisms that are commonly accepted as operating in metal-mediated transformations of alkenes involve the formation of π-complexes as a first step. Examples are hydrogenation reactions, alkene polymerization, olefin metathesis, and nucleophilic attack at olefins. Reactions that involve replacement of a vinyl or aryl hydrogen with another group (e.g., metal-mediated aromatic substitution reactions such as the Heck reaction) are also normally assumed to occur via the initial formation of a π-complex. The fact that C–H activation reactions are observed more frequently with arenes than with saturated hydrocarbons suggests that insertion of a metal into an sp^2 C–H bond proceeds via initial coordination of the metal to the π-electrons adjacent to the C–H bond, followed by its oxidative addition to the metal center (Scheme I).[2]

Scheme I

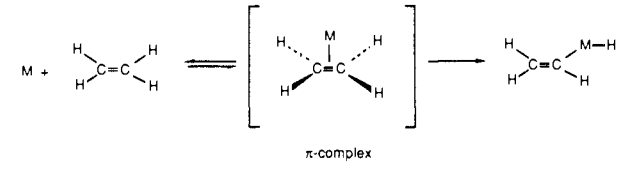

Scheme II

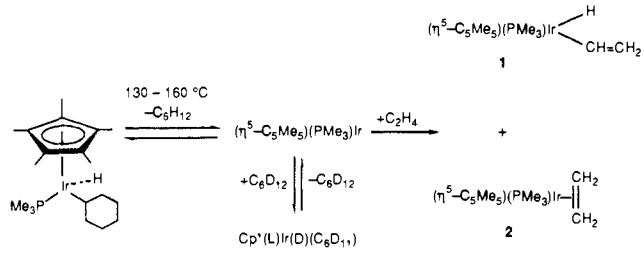

In spite of the fact that most organometallic reactions involving replacement of hydrogen in alkenes or arenes are believed to occur via the intermediacy of π-complexes, it is often difficult to prove conclusively whether this mechanism, rather than direct attack on the C–H bond, operates in a given system. The reason for this is that in most stoichiometric organometallic reactions, either π-complexes or substitution products are formed as stable products; very few processes are known in which these two reaction channels operate simultaneously. However, we recently found that the reactive intermediate "$(\eta^5\text{-}C_5Me_5)(PMe_3)Ir$"[3] forms both the π-complex $(\eta^5\text{-}C_5Me_5)(PMe_3)Ir(H_2C{=}CH_2)$ (**2**) and the C–H oxidative addition product $(\eta^5\text{-}C_5Me_5)(PMe_3)Ir(H)(HC{=}CH_2)$

(1) Collman, J. P.; Hegedus, L. S.; Norton, J. R.; Finke, R. G. *Principles and Applications of Organotransition Metal Chemistry*; University Science Books: Mill Valley, CA, 1987.

(2) (a) Parshall, G. W. *Acc. Chem. Res.* **1970**, *3*, 139. (b) Parshall, G. W. *Acc. Chem. Res.* **1975**, *8*, 113. (c) Parshall, G. W. *Homogeneous Catalysis*; Wiley: New York, 1980; Chapter 7. (d) Muetterties, E. L.; Bleeke, J. R. *Acc. Chem. Res.* **1979**, *12*, 324. (e) Jones, W. D.; Feher, F. J. *J. Am. Chem. Soc.* **1982**, *104*, 4240. (f) Jones, W. D.; Feher, F. J. *J. Am. Chem. Soc.* **1984**, *106*, 1650. (g) Chatt, J.; Davidson, J. M. *J. Chem. Soc.* **1965**, 843–855. (h) Parshall, G. W. *Catalysis* **1977**, *1*, 334. (i) Fryzuk, M. D.; Jones, T.; Einsteln, F. W. D. *Organometallics* **1984**, *3*, 185. (j) Keister, J. B.; Shapley, J. R. *J. Organomet. Chem.* **1975**, *85*, C129. (k) Nubel, P. O.; Brown, T. L. *J. Am. Chem. Soc.* **1984**, *106*, 644.

(3) (a) Janowicz, A. H.; Bergman, R. G. *J. Am. Chem. Soc.* **1983**, *105*, 3929. (b) Bergman, R. G. *Science* **1984**, *223*, 902. We cannot, of course, distinguish between intervention of "free" $(\eta^5\text{-}C_5Me_5)(PMe_3)Ir$ and the corresponding solvated complex, which may in fact be the intermediate in our C–H activation reactions. Throughout this paper we will utilize the former notation for simplicity.

0002-7863/88/1510-5732$01.50/0

Scheme III

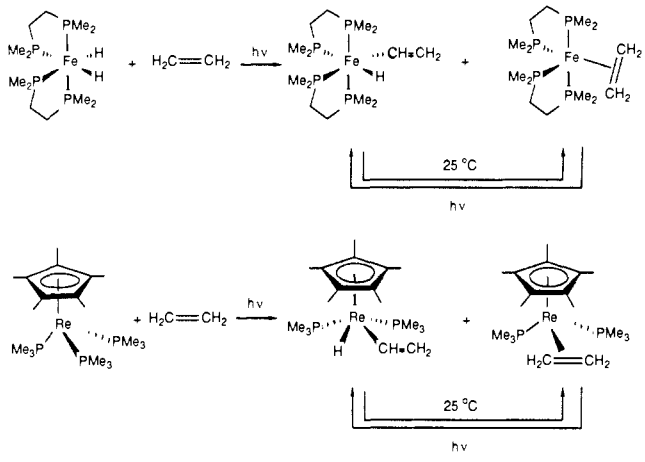

(**1**) on reaction with ethylene. This provided us with an opportunity to examine the two processes operating in competition with one another. Because the π-complex is stable to the C–H insertion reaction conditions, we were able to show rigorously that π-complexation could not, in this system, be a precursor to the C–H insertion product; the two processes must proceed via independent transition states.[4] In this paper, we provide the full details of this work. We also report isotope effect studies designed to illuminate the mechanistic details of both the π-complex formation and C–H insertion reaction pathways. These results provide evidence that an intermediate formed by weak coordination of the C–H bond to the metal center (i.e., a "σ-complex" such as the one we postulated earlier in alkane C–H insertion at rhodium centers[5]) precedes the oxidative addition step.

Results and Discussion

Activation of Ethylene. Thermolysis of the cyclohexyl hydride $(\eta^5\text{-}Me_5C_5)(PMe_3)Ir(C_6H_{11})(H)$ in cyclohexane-d_{12} at 130–160 °C results in reversible formation of $(\eta^5\text{-}Me_5C_5)(PMe_3)Ir$ and cyclohexane.[6] In the presence of ethylene the reactive intermediate can be trapped. This results in formation of $(\eta^5\text{-}Me_5C_5)(PMe_3)Ir(HC{=}CH_2)(H)$ (**1**) and $(\eta^5\text{-}Me_5C_5)(PMe_3)Ir(H_2C{=}CH_2)$ (**2**) in a ratio of 66:34, independent of the reaction temperature, and invariant during the reaction when monitored by ^1H NMR (Scheme II). This is a kinetic product ratio (vide post). The temperature independence of the ratio of **1** to **2** suggests that the two products are formed via two different transition states and that $\Delta\Delta H^{\ddagger}$ is near zero.

Reactions with other olefins are typically more complicated. Use of 2-methylpropene under photochemical conditions results only in C–H bond activation products.[7] Propene appeared to behave similarly to ethylene, but several products were seen, and isolation was not attempted. Use of *cis*- or *trans*-2-butene resulted in a complicated mixture of products and isomerization of the olefin.[8]

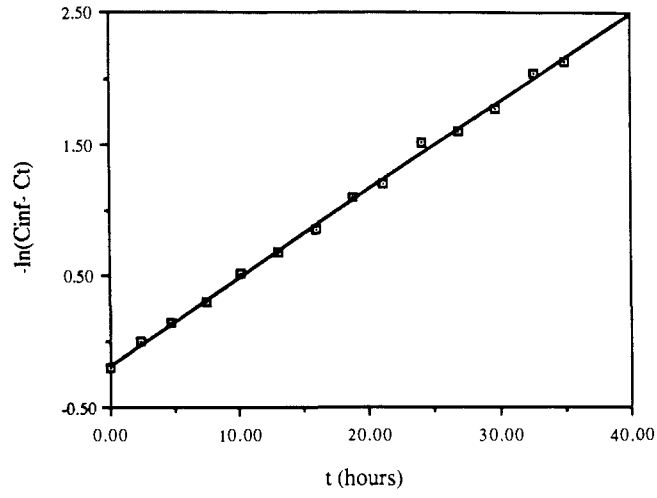

Figure 1. First-order kinetic plot of the thermolysis of $(\eta^5\text{-}Me_5C_5)(PMe_3)Ir(HC{=}CH_2)(H)$ in C_6D_{12} at 185 °C in the presence of 0.05 M PMe_3.

Scheme IV

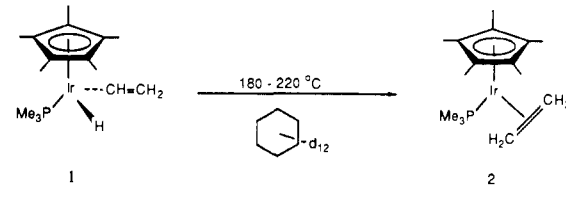

1 2

Before our initial report,[4] several examples were known in which mononuclear transition-metal complexes inserted into the C–H bonds of activated alkenes.[9] In at least one case,[10] changes in olefin substitution resulted in the complete suppression of vinyl hydride formation, and formation of a π-complex. Polynuclear systems are known to insert into the C–H bond of even unactivated alkenes.[11] Here it is believed that coordination to one metal center through the π-electrons "activates" the alkene so that a second metal center can insert into a C–H bond.

Since our initial report,[4] several other mononuclear systems have been discovered which are capable of insertion into the C–H bonds of unactivated alkenes. When "$(DEPE)_2Fe$" (DEPE = $Ph_2PCH_2CH_2PPh_2$) is generated photochemically (at −80 °C) in the presence of ethylene, both the vinyl hydride and the π-complex are formed in a ratio of 90:10 (Scheme III).[12] When the intermediate is generated thermally (−28 °C), by reductive elimination of methane, the ratio is 95:5. Under these conditions, the vinyl hydride exists as a mixture of cis and trans isomers. Raising the temperature to ambient, in either case, results in conversion of the vinyl hydride to the π-complex. Some products arising from C–H activation of the solvent are observed, indicating that some reductive elimination of ethylene is taking place. Irradiation of the π-complex results in a mixture of the vinyl hydride and the π-complex in a ratio of 90:10, indicating that this may be a photostationary state.

Generation of $(\eta^5\text{-}C_5H_5)(PMe_3)_2Re$ at 20 °C in the presence of ethylene results in a 10:1 mixture of the vinyl hydride and the olefin complex (Scheme III).[13] At this temperature, however,

(4) Stoutland, P. O.; Bergman, R. G. *J. Am. Chem. Soc.* **1985**, *107*, 4581.
(5) Perlana, R. A.; Bergman, R. G. *J. Am. Chem. Soc.* **1986**, *108*, 7332.
(6) As the reaction proceeds cyclohexane-d_{12} is incorporated into the iridium complex. On thermolysis in mixed benzene/alkane solvents, $(\eta^5\text{-}Me_5C_5)(PMe_3)Ir(C_6H_{11})(H)$ is converted cleanly and quantitatively to cyclohexane and the benzene C–H activation product $(\eta^5\text{-}Me_5C_5)(PMe_3)Ir(C_6H_5)(H)$. In earlier studies (Buchanan, J. M.; Stryker, J. M.; Bergman, R. G. *J. Am. Chem. Soc.* **1986**, *108*, 1537) we demonstrated that this reaction proceeds by kinetics that are first order in $(\eta^5\text{-}Me_5C_5)(PMe_3)Ir(C_6H_{11})(H)$ and zero order in benzene. The rates are inhibited at high concentration of added cyclohexane. These data are consistent with a mechanism involving reversible, rate-determining reductive elimination of cyclohexane to give "$(\eta^5\text{-}Me_5C_5)(PMe_3)Ir$", followed by trapping of this intermediate by benzene in a subsequent fast step. We assume the same type of mechanism operates with ethylene in place of benzene as the trap.
(7) Reaction of $(\eta^5\text{-}Me_5C_5)(PMe_3)Ir(H)_2$ with 2-methylpropene under photochemical conditions resulted in vinylic C–H insertion products; the reaction was not particularly clean, however. McGhee, W. D., personal communication.
(8) We feel the scrambling is most likely caused by small amounts (<1%) of iridium byproducts formed during the reaction, as there is a slight darkening of the solution.
(9) (a) Komiya, S.; Ito, T.; Cowie, M.; Yamamoto, A.; Ibers, J. A. *J. Am. Chem. Soc.* **1976**, *98*, 3874. (b) Van Baar, J. F.; Vrieze, K.; Stufkens, D. J. *J. Organomet. Chem.* **1975**, *85*, 249. (c) Foot, R. J.; Heaton, B. T. *J. Chem. Soc., Chem. Commun.* **1973**, 838. (d) Aumann, R.; Henkel, G.; Krebs, B. *Angew. Chem., Int. Ed. Engl.* **1982**, *21*, 204.
(10) Tolman, C. A.; Ittel, S. D.; English, A. D.; Jesson, J. P. *J. Am. Chem. Soc.* **1979**, *101*, 1742.
(11) (a) Nubel, P. O.; Brown, T. L. *J. Am. Chem. Soc.* **1984**, *106*, 644. (b) Fryzuk, M. D.; Jones, T.; Einstein, F. W. B. *Organometallics* **1984**, *3*, 185. (c) Keister, J. B.; Shapley, J. R. *J. Organomet. Chem.* **1975**, *85*, C29.
(12) (a) Baker, M. V.; Field, L. D. *J. Am. Chem. Soc.* **1986**, *108*, 7433. (b) Baker, M. V.; Field, L. D. *J. Am. Chem. Soc.* **1986**, *108*, 7436.
(13) Wenzel, T. T.; Bergman, R. G. *J. Am. Chem. Soc.* **1986**, *108*, 4856.

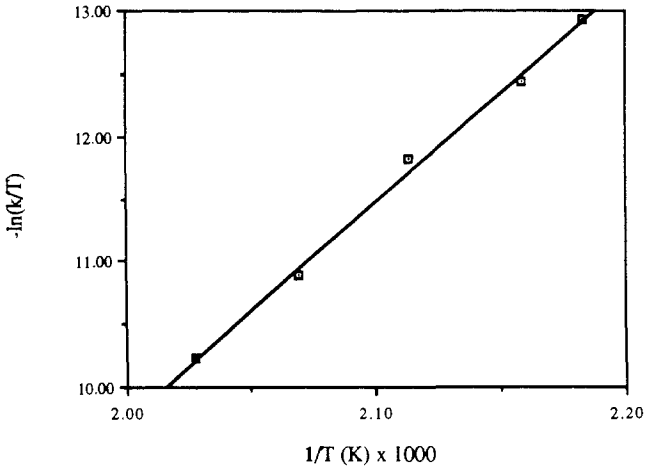

Figure 2. Plot of ln (k/T) vs $1/T$ for the thermolysis of the vinyl complex **1** in cyclohexane-d_{12} at five temperatures between 180 and 220 °C.

the vinyl hydride slowly isomerizes to the π-complex, indicating that the vinyl hydride may be the sole kinetic product. Irradiation of the olefin complex resulted in a 1:6 mixture of it and the vinyl hydride.

Thermolysis of $(\eta^5\text{-}Me_5C_5)(PMe_3)Ir(HC{=}CH_2)(H)$. In our system as well, the η^2-olefin complex is thermodynamically more stable than the vinyl hydride. Thermolysis of pure $(\eta^5\text{-}Me_5C_5)(PMe_3)Ir(HC{=}CH_2)(H)$ in cyclohexane or benzene solvent at temperatures above 180 °C results in quantitative conversion to $(\eta^5\text{-}Me_5C_5)(PMe_3)Ir(H_2C{=}CH_2)$ (Scheme IV). This confirms that the initially observed product mixture arising from activation of ethylene is indeed kinetic rather than thermodynamic. Since $(\eta^5\text{-}Me_5C_5)(PMe_3)Ir(C_6H_5)(H)$ is stable under the thermolysis conditions, its absence when the reaction is performed in benzene indicates that the conversion of **1** to **2** does not occur by reductive elimination to generate *free* (i.e., noncaged) $(\eta^5\text{-}Me_5C_5)(PMe_3)Ir$ and ethylene, followed by addition to the unsaturated metal fragment: if this were occurring, the unsaturated intermediate would be expected to activate benzene.[14] The isomerization of **1** to **2** can be conveniently followed by ^1H NMR in cyclohexane-d_{12} (Figure 1). Using the rates found at five temperatures between 180 and 220 °C allowed us to determine that $\Delta H^{\ddagger} = 34.6 \pm 1.2$ kcal/mol and $\Delta S^{\ddagger} = 2.6 \pm 2.6$ eu (Figure 2). While **1** is quite stable thermally, exposure to small amounts of oxygen resulted in isomerization to **2**.[15] Similarly, if **1** was left in the "gum phase" (the oily residue remaining after removal of the volatiles from the crude reaction mixture), isomerization to **2** was occasionally observed.

From separately conducted calorimetric studies,[16] we can estimate ΔH for the unobserved reductive elimination reaction leading from vinyl hydride **1** to the unsaturated iridium species and free ethylene. In those studies the bond dissociation enthalpies (BDE) of the iridium–hydrogen and iridium–vinyl bonds were found to be 76 and 71 kcal/mol, respectively. Knowing the C–H BDE in ethylene (106 kcal/mol[17a]) allows us to calculate a ΔH of +41 kcal/mol for the reaction. Previously, we estimated that the barrier for the reverse reaction, oxidative addition of $(\eta^5\text{-}Me_5C_5)(PMe_3)Ir$ to a C–H bond, is 2–5 kcal/mol;[16a] this leads to a value of $\Delta H^{\ddagger}$ between 2 and 5 kcal/mol larger than ΔH.[17b]

Scheme V

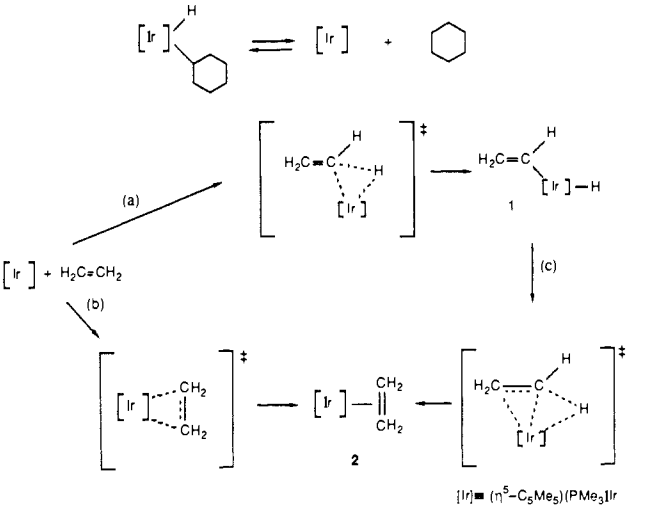

Scheme VI

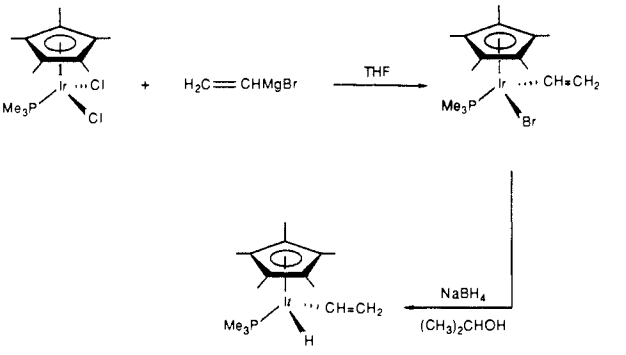

The isomerization of **1** to **2** is thus taking place 6 kcal/mol lower in energy than would be required to fully dissociate ethylene from **1**, and then bring it back to form the π-complex. It is likely that the π-electrons of the vinyl group participate in the **1** → **2** isomerization, lowering this barrier. This is consistent with the general observation that vinyl–alkyl and divinyl transition-metal complexes typically undergo reductive elimination more rapidly than the analogous dialkyl and alkyl–aryl complexes.[18] As summarized in Scheme V, therefore, our data require that three independent pathways are accessible in this system: path a leading from $(\eta^5\text{-}C_5Me_5)(PMe_3)Ir$ to C–H insertion product **1**, path b leading to π-complex **2**, and path c leading from **1** to **2**.[19]

Irradiation of a pure solution of the olefin complex **2** resulted in nearly quantitative regeneration of **1**. Similar cycles have been observed in organic and organometallic systems and formally constitute an energy storage cycle.[20] Analogous cycles have been observed for $(DEPE)_2Fe(HC{=}CH_2)(H)$ and for $(\eta^5\text{-}C_5H_5)(PMe_3)_2Re(HC{=}CH_2)(H)$.[12,13] Irradiation of $(\eta^5\text{-}C_5H_5)Ir(H_2C{=}CH_2)_2$ results in isomerization of only one of the olefin ligands yielding $(\eta^5\text{-}C_5H_5)(H_2C{=}CH_2)Ir(HC{=}CH_2)(H)$.[21]

Independent Synthesis and Structure of Vinyl Hydride 1. In order to confirm the identification of the products from the re-

(14) In competition experiments between benzene and ethylene (vide post), we have determined the relative selectivity between benzene and ethylene to be ca. 1.0.

(15) This was not a controlled oxidation. During an attempted recrystallization of **1** in a Schlenk tube at −40 °C oxygen was apparently introduced into the solution, as $O{=}PMe_3$ was observed. The major organometallic product was **2**. We believe that similar observations made recently in related iridium systems may also be induced by traces of oxygen or other adventitious oxidizing impurities, cf.: Chetcuti, P. A.; Knobler, C. B.; Hawthorne, M. F. *Organometallics* **1988**, *7*, 650.

(16) (a) Nolan, S. P.; Hoff, C. D.; Stoutland, P. O.; Newman, L. J.; Buchanan, J. M.; Bergman, R. G.; Yang, G. K.; Peters, K. S. *J. Am. Chem. Soc.* **1987**, *109*, 3143. (b) Stoutland, P. O.; Bergman, R. G.; Nolan, S. P.; Hoff, C. D. *Polyhedron: Symposium in Print*, in press.

(17) (a) For a recent measurement of this bond energy, and a discussion of values measured earlier, see: Parmar, S. S.; Benson, S. W. *J. Phys. Chem.* **1988**, *92*, 2652. (b) The same value can be calculated with $\Delta H^{\ddagger}$ for reductive elimination of cyclohexane from $(\eta^5\text{-}Me_5C_5)(PMe_3)Ir(C_6H_{11})(H)$, the relevant hydrocarbon C–H BDE's, and the bond dissociation enthalpy of the iridium–cyclohexyl bond (52 kcal/mol).

(18) Chang, J.; Bergman, R. G. *J. Am. Chem. Soc.* **1987**, *109*, 4298 and references therein.

(19) One interesting consequence of these results, as noted by a referee, is that dissociation of ethylene from $(\eta^5\text{-}C_5Me_5)(PMe_3)Ir(C_2H_4)$, if it could be induced to occur thermally, would proceed most rapidly via initial vinylic C–H activation.

(20) Vollhardt, K. P. C.; Weidman, T. W. *J. Am. Chem. Soc.* **1983**, *105*, 1676.

(21) Haddleton, D. M.; Perutz, R. N. *J. Chem. Soc., Chem. Commun.* **1986**, 1734.

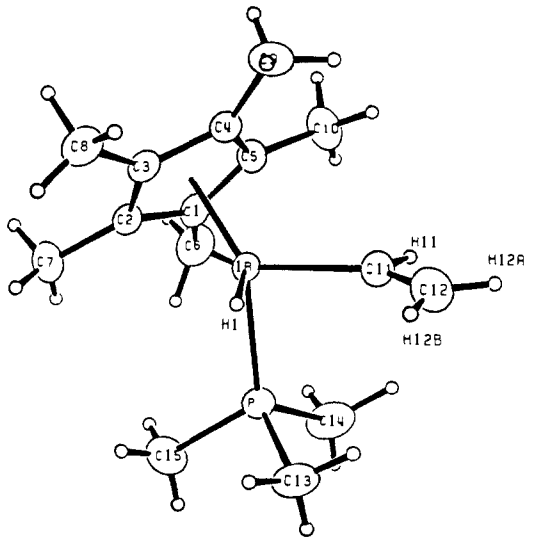

Figure 3. Molecular geometry and labeling for $(\eta^5\text{-}Me_5C_5)(PMe_3)Ir(HC{=}CH_2)(H)$ (**1**). The ellipsoids are scaled to represent the 50% probability surface. Hydrogen atoms are given as arbitrarily small spheres for clarity.

actions with ethylene, and to allow the synthesis of larger quantities of material, we sought independent routes to these compounds. The reaction of $(\eta^5\text{-}Me_5C_5)(PMe_3)Ir(Cl)_2$ with 1.2 equiv of $H_2C{=}CHMgBr$ in THF results in the formation of $(\eta^5\text{-}Me_5C_5)(PMe_3)Ir(HC{=}CH_2)(Br)$ as a yellow/orange, air-stable solid in 67% yield. Reaction of $(\eta^5\text{-}Me_5C_5)(PMe_3)Ir(HC{=}CH_2)(Br)$ with $NaBH_4$ in isopropyl alcohol at a temperature slightly above ambient for several hours yields a white, mildly air-sensitive compound. $(\eta^5\text{-}Me_5C_5)(PMe_3)Ir(HC{=}CH_2)(H)$ was isolated in 83% yield after chromatography at −80 to −100 °C on Alumina (III) under air-free conditions (Scheme VI). Alternatively, **1** may be recrystallized from highly concentrated solutions of pentane or hexamethyldisiloxane. The corresponding deuteride may be made easily by using $NaBD_4$.

We attempted to synthesize $(\eta^5\text{-}Me_5C_5)(PMe_3)Ir(H_2C{=}CH_2)$ in a manner analogous to that mentioned by Maitlis et al.[22] for the synthesis of the analogous PPh_3 complex. Bubbling ethylene through a refluxing ethanol solution of $(\eta^5\text{-}Me_5C_5)(PMe_3)Ir(Cl)_2$ in the presence of Na_2CO_3 for 9 h resulted in a low yield of $(\eta^5\text{-}Me_5C_5)(PMe_3)Ir(H_2C{=}CH_2)$, the major side product being $(\eta^5\text{-}Me_5C_5)(PMe_3)Ir(H)_2$. We have been unable, however, to separate these two compounds cleanly.

We have also carried out an X-ray structure determination of $(\eta^5\text{-}Me_5C_5)(PMe_3)Ir(HC{=}CH_2)(H)$. Clear, yellow needles suitable for diffraction were obtained by slowly cooling a solution of **1** in hexamethyldisiloxane to −40 °C. Fragments cleaved from these crystals were suitable for diffraction and were found to belong to the space group $P2_1/n$. In order to avoid excess thermal motion in the crystal, the data were acquired at −118 °C. In a difference Fourier map, calculated after refinement of all non-hydrogen atoms with anisotropic thermal parameters, peaks corresponding to the expected position of most of the hydrogen atoms were found. A difference Fourier map calculated after inclusion of all other hydrogen atoms clearly showed the position of the hydride. All hydrogen atoms were then allowed to refine with isotropic thermal parameters. The final residuals were R = 2.04% and wR = 2.53%.

The structure shows the expected three-legged piano stool, pseudooctahedral geometry with the cyclopentadienyl ligand occupying three sites and the phosphine, vinyl, and hydride ligands occupying the others (Figures 3 and 4). The Ir–H bond length of 1.61 (5) Å is typical of M–H bond lengths, as is the Ir–C bond length (2.054 (4) Å) which is slightly shorter than that found in $(\eta^5\text{-}Me_5C_5)(PMe_3)Ir(C_6H_{11})$ (2.125 Å), as expected for a bond to an sp^2 carbon. The length of the C=C bond in the vinyl group

(22) Moseley, K.; Kang, J. W.; Maitlis, P. M. *J. Chem. Soc. A* **1970**, 2875.

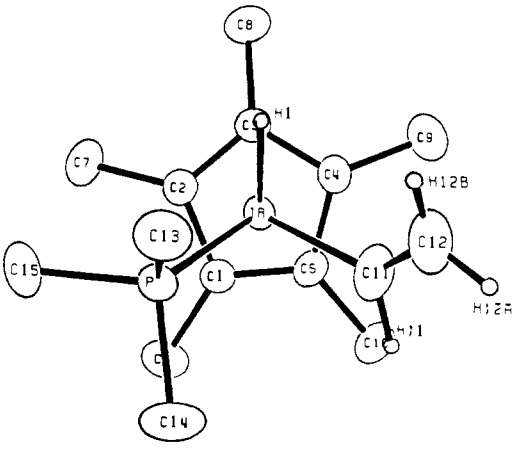

Figure 4. Alternative view of $(\eta^5\text{-}Me_5C_5)(PMe_3)Ir(HC{=}CH_2)(H)$ (**1**) showing orientation of the Ir atom with respect to the centroid of the C_5Me_5 ring.

Table 1. Selected Intramolecular Bond Distances (Å) and esd's for 1.

atoms	distance	atoms	distance
Ir-C_1	2.279(3)	P-C_{14}	1.818(4)
Ir-C_2	2.266(3)	P-C_{15}	1.814(4)
Ir-C_3	2.250(3)	C_1-C_2	1.445(4)
Ir-C_4	2.225(3)	C_2-C_3	1.427(5)
Ir-C_5	2.263(3)	C_3-C_4	1.427(5)
Ir-P	2.226(1)	C_4-C_5	1.453(5)
Ir-C_{11}	2.054(4)	C_5-C_1	1.418(5)
Ir-H_1	1.61(5)	C_1-C_6	1.495(5)
C_{11}-C_{12}	1.296(6)	C_2-C_7	1.496(5)
C_{11}-H_{11}	1.06(5)	C_3-C_8	1.500(5)
C_{12}-H_{12a}	0.96(5)	C_3-C_8	1.500(5)
C_{12}-H_{12b}	0.92(4)	C_4-C_9	1.491(5)
P-C_{13}	1.815(4)	C_5-C_{10}	1.489(5)

Table 2. Selected Intramolecular Bond Angles for 1.

atom 1	atom 2	atom 3	angle (deg)	atom 1	atom 2	atom 3	angle (deg)
Cp_1	Ir	P	135.2	C_5	C_1	C_2	107.9(3)
Cp_1	Ir	C_{11}	123.6	C_1	C_2	C_3	107.6(3)
Cp_1	Ir	H_1	127.4	C_2	C_3	C_4	109.0(3)
P	Ir	C_{11}	85.8(1)	C_3	C_4	C_5	106.9(3)
P	Ir	H_1	82.8(17)	C_4	C_5	C_1	108.5(3)
C_{11}	Ir	H_1	86.2(17)	C_6	C_1	C_2	125.3(3)
Ir	C_{11}	C_{12}	132.8(4)	C_6	C_1	C_5	126 5(3)
Ir	C_{11}	H_{11}	113.7(28)	C_7	C_2	C_1	126.0(3)
H_{11}	C_{11}	C_{12}	113.3(28)	C_7	C_2	C_3	125.7(3)
C_{11}	C_{12}	H_{12a}	117.3(32)	C_8	C_3	C_2	126 0(3)
C_{11}	C_{12}	H_{12b}	121.5(26)	C_8	C_3	C_4	124.8(3)
H_{12a}	C_{12}	H_{12b}	121.1(41)	C_9	C_4	C_3	127.4(3)
Ir	P	C_{13}	116.7(2)	C_9	C_4	C_5	125.5(3)
Ir	P	C_{14}	114.7(2)	C_{10}	C_5	C_1	126.3(3)
Ir	P	C_{15}	117.2(2)	C_{10}	C_5	C_4	125.1(3)

Cp_1 = centroid of the cyclopentadienyl ring.

Table 3. Table of Torsional Angles for 1.

atom 1	atom 2	atom 3	atom 4	angle (deg)
H_1	Ir	C_{11}	C_{12}	-1 9
P	Ir	C_{11}	C_{12}	-84 9
Cp_1	Ir	C_{11}	C_{12}	131.5
C_{11}	Ir	P	C_{15}	-176.1
H_1	Ir	P	C_{13}	-22 8
Cp_1	Ir	P	C_{13}	-160.7
H_1	Ir	Cp_1	C_3	-5.8
H_1	Ir	Cp_1	C_4	65 7
C_{11}	Ir	Cp_1	C_4	-48.3
C_{11}	Ir	Cp_1	C_5	24 6
P	Ir	Cp_1	C_1	-27.1
P	Ir	Cp_1	C_2	45.4

Cp_1 = centroid of the cyclopentadienyl ring

(1.296 Å) is slightly shorter than that of a typical double bond. The pentamethylcyclopentadienyl ligand is nearly planar, but there is a small, but statistically significant, variation (6 σ) in the C–C bond lengths. The shortest C–C bond (1.418 Å), C_1–C_5, is opposite the hydride ligand. Adjacent to it are the two longest bonds, C_1–C_2 and C_4–C_5, at 1.445 and 1.453 Å, respectively. The remaining C–C bonds, C_2–C_3 and C_3–C_4, are of intermediate length at 1.427 Å. Selected bond lengths and angles are given in Tables 1 and 2. Selected torsional angles are given in Table 3. These data show that the Ir atom is displaced toward C1 and C5 of the C_5Me_5 ring, indicating a significant contribution from an allyl–ene

resonance structure. Similar, but larger, deviations have been observed for $(\eta^5\text{-}Me_5C_5)Rh(CO)_2$[23] and $(\eta^5\text{-}Me_5C_5)Co(CO)_2$.[24] It is thought that this is caused by a localization of the p_π electron density on the cyclopentadienyl ligand, believed to arise from a breakdown of the doubly degenerate e_1 ring orbital degeneracy caused by interaction with nondegenerate metal-based atomic orbitals.

Intermolecular Isotope Effects. By measuring the relative rates of reaction of $(\eta^5\text{-}Me_5C_5)(PMe_3)Ir(C_6H_{11})(H)$ with ethylene and with deuterium-labeled ethylenes, one can determine the intermolecular isotope effect for both C–H insertion and π-complex formation. To measure the intermolecular isotope effect we first allowed the iridium species to compete for ethylene and ethylene-d_n in the same tube and attempted to measure the final relative concentrations of **1** and **1**-d_n in order to calculate relative rates. This required making a comparison between the cyclopentadienyl or the PMe_3 resonances and the vinyl resonances. Unfortunately, the errors incurred in determining the relative amounts of **1** and **1**-d_n in this manner were unacceptably large. Attempts to take advantage of the splitting in the ^{31}P NMR spectrum caused by a deuterium on the metal were similarly unsuccessful. A further complication should be noted here. While experimenting with reactions in which ethylene and ethylene-d_4 were heated in the same tube in the presence of $(\eta^5\text{-}Me_5C_5)(PMe_3)Ir(C_6H_{11})(H)$, it was found that the ethylenes underwent H/D exchange with each other. Mass spectral analysis of the volatile materials showed a nearly statistical mixture of d_0, d_1, d_2, d_3, and d_4 ethylenes. Later experiments (vide post) revealed that this scrambling process was also observed with ethylene-d_2. Addition of a small amount of PMe_3 (>0.05 M) to the reaction mixture effectively inhibited this (4–20% scrambled) so that any scrambling had a negligible influence on the isotope effects.[25] Interestingly $P(C_6H_5)_3$ was not effective at stopping this scrambling process. All experiments aimed at determining isotope effects (both intra- and intermolecular competition experiments) were thus done in the presence of at least 0.05 M PMe_3.

In order to determine the intermolecular isotope effect we sought a reagent that could be mixed with ethylene and ethylene-d_n in separate tubes, compete with ethylene for the metal center, and lead to a product with a signal in the NMR spectrum sufficiently different from those of $(\eta^5\text{-}Me_5C_5)(PMe_3)Ir(HC{=}CH_2)(H)$ and $(\eta^5\text{-}Me_5C_5)(PMe_3)Ir(H_2C{=}CH_2)$ so that accurate integrations could be made. In this way, the relative rates of reaction of ethylene/ethylene-d_n vs this reagent could be measured, thus allowing us to directly compare the rates of reaction with ethylene and with ethylene-d_n, as if they were competing for the iridium center in the same tube. Benzene proved to be suitable for this as it was stable to the reaction conditions and reacts with the iridium center forming the stable phenyl hydride complex, which has a distinct ^{31}P NMR shift.

We thus made up a standard solution of $(\eta^5\text{-}Me_5C_5)(PMe_3)Ir(C_6H_{11})(H)$ and C_6H_6 in cyclohexane-d_{12} and split this between two NMR tubes so that the volume of solution in each tube was the same. We condensed $H_2C{=}CH_2$ into one of the tubes and into the other an equal amount of $D_2C{=}CD_2$. In order to be sure that the pressure of ethylene (and thus the concentration in solution) was the same in each tube, the tubes were sealed so that the lengths were equal (within 3 mm, total length ca. 25 cm). Side-by-side thermolysis at 145 °C of these tubes resulted in the first containing $(\eta^5\text{-}Me_5C_5)(PMe_3)Ir(C_6H_5)(H)$, $(\eta^5\text{-}Me_5C_5)(PMe_3)Ir(HC{=}CH_2)(H)$, and $(\eta^5\text{-}Me_5C_5)(PMe_3)Ir(H_2C{=}CH_2)$ and the second containing $(\eta^5\text{-}Me_5C_5)(PMe_3)Ir(C_6H_5)(H)$, $(\eta^5\text{-}Me_5C_5)(PMe_3)Ir(DC{=}CD_2)(D)$, and $(\eta^5\text{-}Me_5C_5)(PMe_3)Ir(D_2C{=}CD_2)$. In Figures 5 and 6 are shown representative ^{31}P NMR spectra of the reaction mixtures at the end of the reaction.

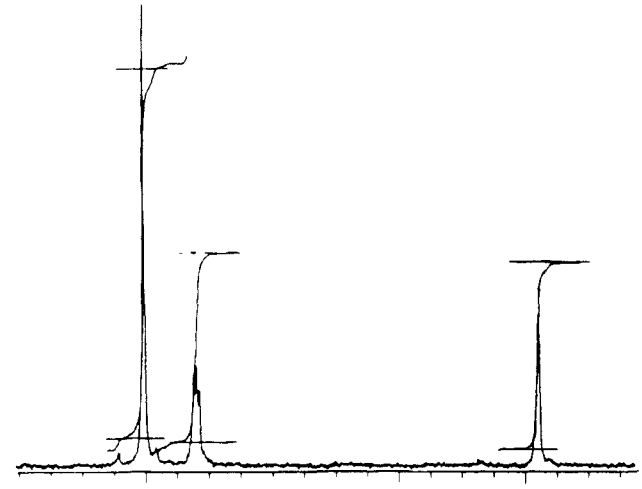

Figure 5. ^{31}P NMR spectrum of the reaction mixture resulting from thermolysis of $(\eta^5\text{-}Me_5C_5)(PMe_3)Ir(C_6H_{11})(H)$ in the presence of $H_2C{=}CH_2$ and C_6H_6. Assignments (left to right; chemical shifts referred to 85% H_3PO_4): $(\eta^5\text{-}Me_5C_5)(PMe_3)Ir(C_6H_5)(H)$, δ −41.15; $(\eta^5\text{-}Me_5C_5)(PMe_3)Ir(HC{=}CH_2)(H)$, δ −42.09; $(\eta^5\text{-}Me_5C_5)(PMe_3)Ir(H_2C{=}CH_2)$, δ −47.36.

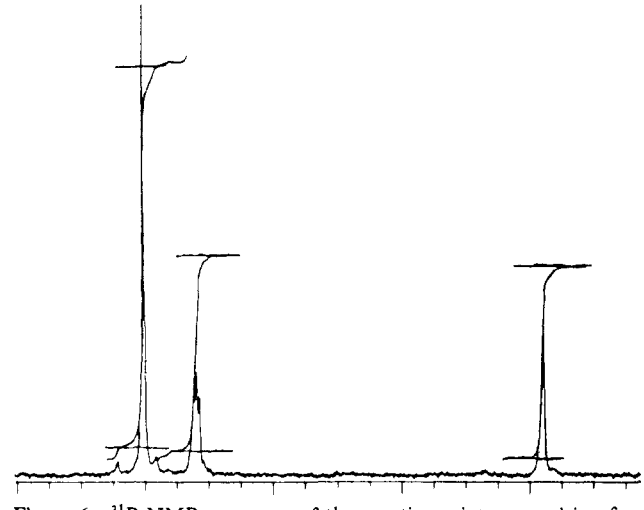

Figure 6. ^{31}P NMR spectrum of the reaction mixture resulting from thermolysis of $(\eta^5\text{-}Me_5C_5)(PMe_3)Ir(C_6H_{11})(H)$ in the presence of $D_2C{=}CD_2$ and C_6H_6. Assignments (left to right): $(\eta^5\text{-}Me_5C_5)(PMe_3)Ir(C_6H_5)(H)$, $(\eta^5\text{-}Me_5C_5)(PMe_3)Ir(DC{=}CD_2)(D)$, and $(\eta^5\text{-}Me_5C_5)(PMe_3)Ir(D_2C{=}CD_2)$. Chemical shifts are given in the caption to Figure 5.

Scheme VII

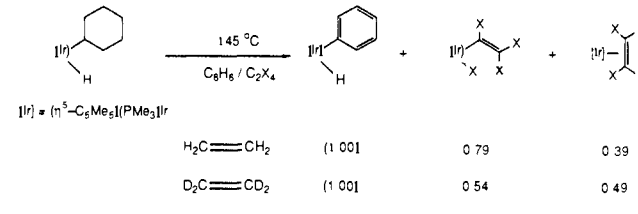

Since the concentration of benzene is the same in both tubes, the rate of formation of $(\eta^5\text{-}Me_5C_5)(PMe_3)Ir(C_6H_5)(H)$ is the same in both tubes. This allowed us to normalize the concentrations of the products formed in each tube to the amount of $(\eta^5\text{-}Me_5C_5)(PMe_3)Ir(C_6H_5)(H)$ formed, and to compare the relative amounts (and thus the relative rates of formation) of $(\eta^5\text{-}Me_5C_5)(PMe_3)Ir(HC{=}CH_2)(H)$ with $(\eta^5\text{-}Me_5C_5)(PMe_3)Ir(DC{=}CD_2)(D)$, and of $(\eta^5\text{-}Me_5C_5)(PMe_3)Ir(H_2C{=}CH_2)$ with $(\eta^5\text{-}Me_5C_5)(PMe_3)Ir(D_2C{=}CD_2)$ (Scheme VII).

In this way we were able to determine the intermolecular isotope effect for insertion into a C–H bond, and for formation of the π-complex. Finding the intermolecular isotope effect k_H/k_D for

(23) Lichtenberger, D. L.; Blevins, C. H., II.; Ortega, R. B. *Organometallics* **1984**, *3*, 1614.
(24) Byers, L. R.; Dahl, L. F. *Inorg. Chem.* **1980**, *19*, 277.
(25) It seems likely that the scrambling is caused by adventitious metal-containing impurities (cf. ref 15) which PMe_3 is able to scavenge. We have shown in other systems that the rate of reductive elimination in $(\eta^5\text{-}C_5Me_5)(PMe_3)Ir(R)(H)$ complexes is independent of the concentration of added PMe_3: cf. ref 6.

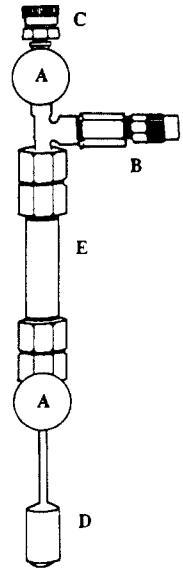

Figure 7. Apparatus used to measure the relative solubilities of $H_2C{=}CH_2$ and $D_2C{=}CD_2$: (A) Nupro valves, (B) pressure release valve, (C) Cajon Ultra-Torr fitting, (D) stainless steel bomb, (E) stainless steel tubing.

formation of **1** is straightforward when $H_2C{=}CH_2$ is compared to $D_2C{=}CD_2$, as there are no statistical corrections to make. When the rate of insertion into any of the d_2 ethylenes is compared to ethylene, however, statistical factors must be taken into account in deriving the isotope effects. We define the rate of insertion into one C–H bond of $H_2C{=}CH_2$ to be k_H. The total rate of insertion into $H_2C{=}CH_2$ is then $4k_H$, and the total rate of insertion into the C–H(D) bonds of ethylene-d_2 (assuming for simplicity that secondary isotope effects are negligible) is $2k_H + 2k_D$. Knowing the relative rates of insertion into ethylene and ethylene-d_2 one can thus solve for k_H/k_D. Propagation of errors in solving for k_H/k_D, however, makes the uncertainty in k_H/k_D large (0.2–0.3). The values we found were consistent with this. While they were centered on the value found with ethylene and ethylene-d_4 (where the comparison is simple, $4k_H$ vs $4k_D$), they varied considerably and therefore are not included in our final value for the intermolecular isotope for insertion in a C–H bond. Comparing rates of reaction of $H_2C{=}CH_2$ with those for $D_2C{=}CD_2$ gave intermolecular isotope effects of 1.45, 1.46, and 1.55 ± 0.15 (error based on estimated 5% reproducibility in NMR integration). Averaging these values resulted in a final value of $k_H/k_D = 1.49 \pm 0.08$.

Similarly, the intermolecular isotope effect on formation of π-complex **2** can be determined. If we assume the transition state for formation of the π-complex involves a symmetrical interaction of iridium with the π-electrons, the isotope effect will consist entirely of a secondary effect where $k_D = \delta^n k_H$, with n = number of deuterium atoms on the ethylene, if δ is the effect that each deuterium has on the rate. For the three experiments the relative ratios of **2** to **2**-d_4 were found to be 0.81, 0.80, and 0.84 ± 0.08. Averaging these values results in $k_H/k_D = 0.82 \pm 0.05$. The effect of one deuterium, δ, is thus $(k_H/k_D)^{1/4} = 0.95 \pm 0.02$.

The accuracy of the intermolecular isotope effects also depends on there being equal ratios of benzene and of ethylene or ethylene-d_4 in each tube. We are confident that the amounts of benzene in each tube are the same as the tubes were filled from a standard solution. The amount of ethylene in each tube, however, depended on $H_2C{=}CH_2$ and $D_2C{=}CD_2$ having the same solubility in cyclohexane. While we did not initially expect there to be any significant difference, earlier measurements have indicated that liquid ethylene-d_4 has a slightly higher vapor pressure (3%) than ethylene.[26] We thus elected to measure the relative solubilities.

(26) Bigeleisen, J.; Ribnikar, S. V.; Van Hook, W. A. *J. Chem. Phys.* **1963**, *38*, 489.

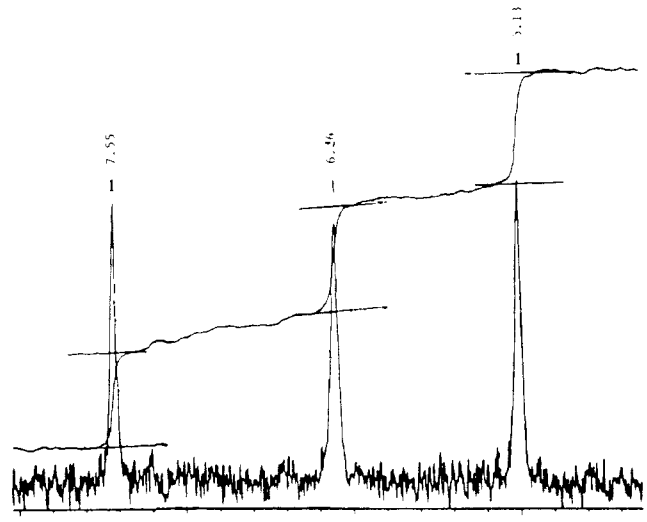

Figure 8. Vinyl region of the ^2H NMR spectrum of a reaction mixture resulting from thermolysis of $(\eta^5\text{-}Me_5C_5)(PMe_3)Ir(C_6H_{11})(H)$ in the presence of ethylene-*1,1*-d_2.

Scheme VIII

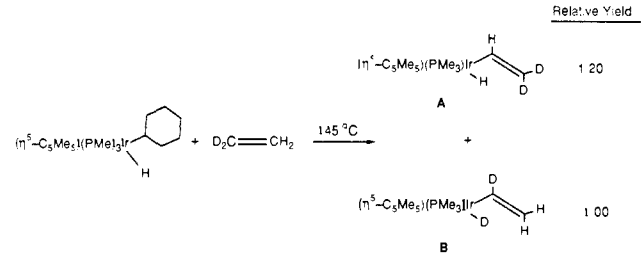

We measured the relative solubilities using the apparatus shown in Figure 7. Briefly, it consists of a stainless steel bomb fitted to a stainless steel pipe with a valve. At the other end of the pipe is another valve with a fitting for attachment to a vacuum line. The bomb was filled with cyclohexane and thoroughly degassed (freeze–pump–thawed 5 to 10 times). A known amount of ethylene was then condensed into the apparatus, the top valve closed, and the apparatus allowed to warm to room temperature over 2 to 3 h. Closure of the lower valve resulted in nearly all of the ethylene below it being dissolved in the cyclohexane (9.4 mL of cyclohexane in the 11.2 mL lower section). Using a vacuum line and a Toepler pump, we then measured the gas above the lower valve, which is inversely related to the amount in solution. These results show an insignificant difference ($D_2C{=}CD_2$ is 2 ± 4% more soluble) in the solubility of ethylene and ethylene-d_4 in cyclohexane under these conditions. We did not correct the isotope effects for this slight difference. Details of the experimental procedure and the actual solubilities are given in the Experimental Section.

Intramolecular Isotope Effects. Thermolysis of $(\eta^5\text{-}Me_5C_5)(PMe_3)Ir(C_6H_{11})(H)$ at 145 °C in cyclohexane-d_{12} in the presence of each of the isomers of ethylene-d_2 (ethylene-*1,1*-d_2, *cis*-ethylene-*1,2*-d_2, and *trans*-ethylene-*1,2*-d_2) allowed observation of the competition between insertion into a C–H or into a C–D bond in the same molecule (an intramolecular isotope effect). For example, reaction with ethylene-*1,1*-d_2 results in a mixture of $(\eta^5\text{-}Me_5C_5)(PMe_3Ir(DC{=}CH_2)(D)$ (**B**) and $(\eta^5\text{-}Me_5C_5)(PMe_3)Ir(HC{=}CD_2)(H)$ (**A**). The use of ^2H NMR allowed us to determine the relative amounts of deuterium in each position, thus allowing us to determine the relative amounts of **A** and **B** formed (Scheme VIII). In Figure 8 is shown a representative ^2H NMR spectrum of the vinyl region.

In three separate reactions with ethylene-*1,1*-d_2 we observed that the ratio of **A** to **B** was independent of the length of the thermolysis (between 10 and 24 h), suggesting that the ratio observed was under kinetic control. This did not preclude, however, a fast process (compared to the overall reaction rate) in which

Table 4. Intramolecular Isotope effects for formation of 1.

Ethylene-d_2	k_H/k_D
ethylene-1,1-d_2	1.13 1.20 1.20
cis-ethylene-1,2-d_2	1.17
trans-ethylene-1,2-d_2	1.21

hydrogen and deuterium atoms were exchanged between the vinyl group and the metal.[27] In this case the ratio of **A** to **B** would reflect a thermodynamic isotope effect. In order to examine this possibility, we synthesized $(\eta^5\text{-}Me_5C_5)(PMe_3)Ir(HC{=}CH_2)(D)$, to look for exchange of the deuterium label into the vinyl group. Thermolysis at temperatures up to those at which conversion to **2** took place revealed no scrambling of the deuterium into the β-position of the vinyl group, as determined by ^2H NMR. A small amount of scrambling into the α-position (<10%) was occasionally observed. This was not uniformly repeatable, and we therefore conclude it is a process catalyzed by adventitious impurities. This result indicates that the position of the deuterium in $(\eta^5\text{-}Me_5C_5)(PMe_3)Ir(HC{=}CH_2)(D)$ is not under thermodynamic control, and the intermolecular isotope distribution is kinetically determined.

Because the products are formed under kinetic control, the final relative concentrations of **A** and **B** can be used to calculate the relative rates of insertion into the C–H and C–D bonds. In Table 4 the intramolecular isotope effects are compiled for reaction of the three ethylene-d_2 isomers. Surprisingly, the values are identical within our experimental uncertainty; the implications of this result are discussed below.

We found that if care was taken, each integration of the ^2H NMR was repeatable to ±5%. This leads to an error in k_H/k_D for each experiment of ±0.08. We gained further confidence in our numbers by making sure that each experiment was internally consistent. To do this we integrated the different vinyl resonances against each other, and against the hydride resonance. Within experimental error, the isotope effects were independent of the resonances chosen for comparison.[28] Comparisons between the vinyl resonances typically showed less scatter, and thus were used for the k_H/k_D values shown in Table 4. Averaging the values shown reduces our random error, resulting in a final value of 1.18 ± 0.03.

Discussion of Isotope Effects

Intermolecular Effects. The intermolecular isotope effects we observed are kinetic isotope effects, as the products are completely stable to the reaction conditions. The effects are much smaller than typical maximum values for primary kinetic isotope effects, but are consistent with other observations. The isotope effect observed upon oxidative addition of cyclohexane to $(\eta^5\text{-}Me_5C_5)(PMe_3)Ir$ was found to be 1.38.[29] The intermolecular isotope effect for insertion into a C–H bond of benzene by $(\eta^5\text{-}Me_5C_5)(PMe_3)Rh$ was found to be 1.05.[30] In this case, it was discovered that the intramolecular isotope effect (found by using benzene-*1,2,3*-d_3) was significantly larger (1.4). Small isotope effects such as these have typically been considered to be associated with either a very early transition state, in which little C–H bond breakage has occurred, or with a nonlinear transition state. It is difficult to predict the geometry of the transition state, but the high exothermicity of the C–H insertion reaction between $(\eta^5\text{-}Me_5C_5)(PMe_3)Ir$ and $H_2C{=}CH_2$ (ca. 40 kcal/mol) is consistent with an early transition state.

As no C–H bonds are broken in the formation of $(\eta^5\text{-}Me_5C_5)(PMe_3)Ir(H_2C{=}CH_2)$, the isotope effect observed is a secondary effect. Secondary effects are typically caused by rehybridization of C–H bonds, which when changing from sp^2 to sp^3 results in a loosening of the C–H bending modes.[31] This change in the bending frequency is different for C–H and C–D bonds, giving rise to an isotope effect. The carbons in the ethylene ligand of $(\eta^5\text{-}Me_5C_5)(PMe_3)Ir(H_2C{=}CH_2)$ are not sp^3 hybridized, but they are probably significantly perturbed from free ethylene. The X-ray structure of a related compound, $(\eta^5\text{-}Me_5C_5)(P(C_6H_5)_3)Rh(H_2C{=}CH_2)$,[32] shows a lengthening of the C–C bond, and a bending back of the C–H bonds, consistent with a significant contribution from a metallacyclopropane resonance form. Our spectroscopic data are consistent with this formulation.

The size of the isotope effect observed when sp^2 carbons are changing to sp^3 carbons depends on the nature of the transition state, and on the number of hydrogen atoms attached to the carbon undergoing rehybridization. Reasonable estimates can often be made for simple systems by considering the changes in the bending force constants.[30] Some literature precedent for organometallic systems is available, but the values known are thermodynamic (K_H/K_D as opposed to k_H/k_D) isotope effects. For example, the equilibrium isotope effect for the complexation/elimination of ethylene/ethylene-d_4 from Ag^+ was found to be 0.89 (i.e., ethylene-d_4 is more strongly complexed to Ag^+).[33] Since interactions of alkenes with Ag^+ consist almost entirely of donation of electron density from the alkene to the metal center, it is likely that the ethylene structure is perturbed only slightly from that found in the free ligand. If it were possible to measure the thermodynamic isotope effect for binding of ethylene/ethylene-d_4 to $(\eta^5\text{-}Me_5C_5)(PMe_3)Ir$, it would undoubtedly be larger.

Comparison of Inter- and Intramolecular Isotope Effects. The values found for the isotope effect for insertion into a C–H bond are similar to those found earlier for alkanes; the distinguishing factor, however, is that the inter- and intramolecular kinetic isotope effects are not equivalent. Assuming this difference is not due to a peculiar secondary isotope effect of the non-reacting C–D bonds, this non-equivalence requires an intermediate on the reaction pathway from which partitioning can occur. In the present case, this means that there is an intermediate having the stoichiometry $[(\eta^5\text{-}Me_5C_5)(PMe_3)Ir{\cdot}(H_2C{=}CH_2)]$, which (a) is not the π-complex **2**, (b) is formed upon reaction with ethylene (an intermolecular reaction), and (c) can then go on to insert the metal center into any of the four C–H bonds (a unimolecular, intramolecular reaction).

This accommodates having different intra- and intermolecular isotope effects in the following way. In the first step $(\eta^5\text{-}Me_5C_5)(PMe_3)Ir$ can compete for any of the ethylenes present. The relative rate of formation of insertion products formed with $H_2C{=}CH_2$ and $D_2C{=}CD_2$ will be affected by the rate of reaction with ethylene/ethylene-d_4 (the intermolecular step), and/or the rate of the actual insertion (the intramolecular step), depending on the relative rates. An intermolecular competition experiment thus potentially provides information on both steps of the reaction. When a partially labeled ethylene such as ethylene-d_2 is used, only one intermediate $[(\eta^5\text{-}Me_5C_5)(PMe_3)Ir{\cdot}(C_2H_2D_2)]$ can result. This, however, can lead to both C–H and C–D insertion products. The isotope effect observed with a partially deuteriated ethylene thus reflects the isotope effect of the second step. Our system is more complex than this, however, as isotopic substitution also affects another pathway, formation of $(\eta^5\text{-}Me_5C_5)(PMe_3)Ir(H_2C{=}CH_2)$.

As mentioned above,[30] different inter- and intramolecular isotope effects were also observed in the reaction of benzene with $(\eta^5\text{-}Me_5C_5)(PMe_3)Rh$. In this case the intermolecular isotope effect was very small (1.05), indicating that little C–H bond

(27) Similar rearrangements have been observed in this and other systems. (a) Paper cited in footnote 6. (b) Erker, G. *Acc. Chem. Res.* **1984**, *17*, 103.

(28) For experiments with ethylene-*1,1*-d_2, the ratio of **A** to **B** (Scheme VIII) can be determined by comparing the α-deuterium to either β-deuterium, or by comparing the deuteride to either β-deuterium.

(29) See ref 3a; isotope effects of similar magnitude have been observed in the rhodium series (ref 5 and 30).

(30) Jones, W. D.; Feher, F. J. *J. Am. Chem. Soc.* **1986**, *108*, 4814.

(31) (a) Lowry, T. H.; Richardson, K. S. *Mechanism and Theory in Organic Chemistry*; Harper and Row: New York, 1981; Chapter 2. (b) Streitweiser, A., Jr.; Lagow, R. H.; Fahey, R. C.; Suzuki, S. *J. Am. Chem. Soc.* **1958**, *80*, 2326.

(32) Porzio, W.; Zocchi, M. *J. Am. Chem. Soc.* **1978**, *100*, 2048.

(33) Cvetanovic, R. J.; Duncan, F. J.; Falconer, W. E.; Irwin, R. S. *J. Am. Chem. Soc.* **1965**, *87*, 1827. See also: Schurig, V. V. *Chem. Z.* **1977**, *101*, 173 and references therein.

Scheme IX

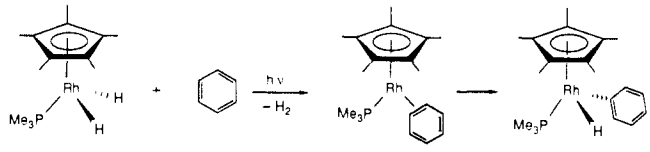

Scheme X

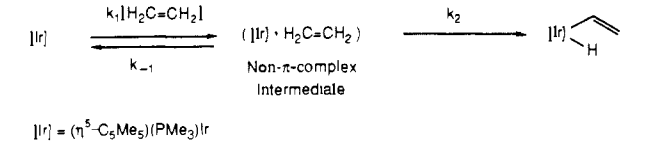

Scheme XI

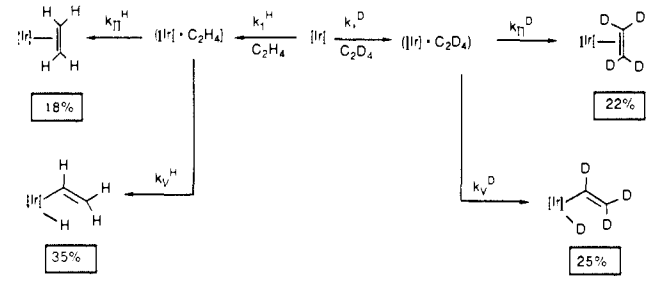

breakage was occurring in the first step. Use of benzene-*1,3,5-d*$_3$ allowed determination of the isotope effect for the second step, insertion into the C–H bond. This isotope effect was found to be larger, $k_H/k_D = 1.4$. It was proposed that the first step resulted in production of an η^2-arene complex. Such a complex would have C–H bonds very similar to those found in benzene, and this could account for the small isotope effect observed. The second step would then involve insertion into one of the C–H bonds, which would be expected to have a larger isotope effect as a C–H bond was being broken (Scheme IX). *In our system, however, the corresponding π-complex cannot be an intermediate—it is stable to the reaction conditions.* Later we will return to the nature of the intermediate in our system.

Since two products are formed in the activation of ethylene by iridium, the analysis of the isotope effects is more complex, but potentially more informative. The significance of the intermolecular isotope effect is not clear because we do not know (referring to Scheme X) if it reflects (a) just the selectivity of the first step (k_1 rate determining), (b) the selectivity of the first step and the insertion step (k_{-1} and k_2 competitive), or (c) the thermodynamic selectivity of the first step followed by the insertion step (a preequilibrium k_1/k_{-1}, followed by a rate-determining step k_2). By combining the information from the intermolecular competition experiment with the isotope effect for π-complex formation and the intramolecular isotope effect, we can determine the effect of isotopic substitution on each step of potential reaction mechanisms. Any reaction mechanism we might consider must at least satisfy the requirement that an intermediate lies on the reaction pathway leading to (η^5-Me_5C_5)(PMe_3)Ir(HC=CH_2)(H).

Two possible mechanisms are shown in Schemes XI and XII. Let us first consider mechanism A. Here the intermediate formed upon reaction of ethylene with (η^5-Me_5C_5)(PMe_3)Ir can go on to insert into any of the C–H bonds or can form the π-complex. Summarized in Scheme XI are the rate constants involved in this mechanism, and the relative amounts of products formed in the intermolecular competition experiment. Comparing the relative amounts of products derived from reaction with H_2C=CH_2 with those from reaction with D_2C=CD_2 allows us to determine the isotope effect (k_1^H/k_1^D) for the first step in the reaction (eq 1).

$$[k_1^H/k_1^D] = (18 + 35)/(22 + 25) = 1.16 \qquad (1)$$

From the intramolecular competition experiment we know that the isotope effect associated with insertion into a C–H(D) bond (k_V^H/k_V^D) is 1.18. This allows us to determine the isotope effect

Scheme XII

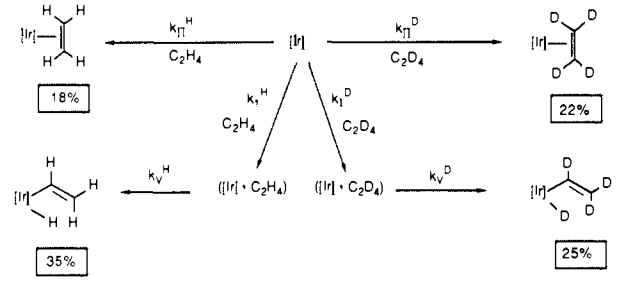

Table 5. A summary of the individual isotope effects for Mechanisms **A** and **B**.

Step	k_H/k_D (Mech. A)	k_H/k_D (Mech. B)
k_1	1.16	1.49
k_V	1.18	1.18
k_π	0.64	0.80

associated with formation of the π-complex from the intermediate (k_π^H/k_π^D). Because we know how the intermediate partitions between (η^5-Me_5C_5)(PMe_3)Ir(HC=CH_2)(H) and (η^5-Me_5C_5)(PMe_3)Ir(H_2C=CH_2) (k_V/k_π), we can solve for $[k_H/k_D]_\pi$ in the following way (eq 2–5).

$$([k_H]_V/[k_H]_\pi)([k_D]_\pi/[k_D]_V) = (35/18)(22/25) = 1.84 \qquad (2)$$

$$(k_V^H/k_V^D)(k_\pi^D/k_\pi^H) = 1.84 \qquad (3)$$

$$(1.18)(k_\pi^D/k_\pi^H) = 1.84 \qquad (4)$$

$$(k_\pi^H/k_\pi^D) = 0.64 \qquad (5)$$

Mechanism B is distinct from mechanism A in that (η^5-Me_5C_5)(PMe_3)Ir(H_2C=CH_2) is formed directly from (η^5-Me_5C_5)(PMe_3)Ir and H_2C=CH_2 in mechanism B. In Scheme XII are again summarized the appropriate rate constants and relative amounts of products found in the intermolecular competition experiment. Here, as in mechanism A, the intramolecular isotope effect $k_V^H/k_V^D = 1.18$. In this case, however, the isotope effect on formation of (η^5-Me_5C_5)(PMe_3)Ir(H_2C=CH_2) is simply the amount of (η^5-Me_5C_5)(PMe_3)Ir(H_2C=CH_2) (18%) divided by the amount of (η^5-Me_5C_5)(PMe_3)Ir(D_2C=CD_2) (22%): $k_\pi^H/k_\pi^D = 0.80$. Similarly, the isotope effect on formation of the intermediate (k_1^H/k_1^D) is simply the ratio of (η^5-Me_5C_5)(PMe_3)Ir(HC=CH_2)(H) to (η^5-Me_5C_5)(PMe_3)Ir(DC=CD_2)(D): $k_1^H/k_1^D = 35/25 = 1.49$. A summary of the isotope effects derived for mechanism A and B is give in Table 5. It is possible in either mechanism that the k_1 step is reversible. If k_{-1} were sufficiently fast, the isotope effect found for the first step would not be a kinetic isotope effect but a thermodynamic effect.

It is difficult to distinguish rigorously between mechanisms A and B. However, we prefer mechanism A for two reasons. First, it is unusual enough to have to postulate a mechanism in which π-complex formation and C–H insertion must take place via two different transition states; mechanism **B** requires, in addition, that the route to π-complex **2** is independent of the [Ir]·C_2H_4 intermediate. We are therefore more comfortable with a hypothesis in which some conversion of the intermediate into the π-complex is allowed, as it is in mechanism A. Second, as mentioned above in the analysis of mechanism A, the isotope effect on the complex-formation step, k_1^H/k_1^D, is calculated to be 1.16 for this pathway, whereas in mechanism B the complex-formation isotope effect is much larger (1.49). Because this step presumably involves only weak interaction of the metal center with the C–H bond, it seems more reasonable that it be characterized by the smaller isotope effect.

Nature of the Intermediate. From thermochemical and kinetic experiments discussed earlier, we can make good estimates for the energy of the (η^5-C_5Me_5)(PMe_3)Ir intermediate relative to the starting materials and products. The energetic situation is summarized in Figure 9. Our calorimetric studies (vide supra) suggest that (η^5-Me_5C_5)(PMe_3)Ir(HC=CH_2)(H) lies 41 kcal/mol lower in energy (ΔH) than (η^5-Me_5C_5)(PMe_3)Ir and free ethylene. The small kinetic selectivities we observe for the intermediate

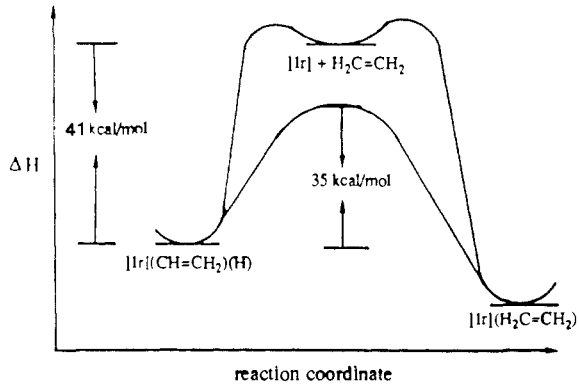

Figure 9. Proposed approximate reaction coordinate diagram for the reaction of "(η^5-Me_5C_5)(PMe_3)Ir" with ethylene, and the conversion of **1** to **2**.

suggest to us that the barrier for oxidative addition is 2–5 kcal/mol. Our activation energy experiments require that the transition state leading from **1** to **2** lies 35 kcal/mol above **1**. Furthermore, upon thermolysis of (η^5-Me_5C_5)(PMe_3)Ir(HC=CH_2)(D), no scrambling of the deuterium into the vinyl group is seen up to temperatures at which conversion to **2** is seen. This indicates that the intermediate responsible for the different inter- and intramolecular isotope effects must lie *higher* than 35 kcal/mol above **1** (Figure 9).

The potential energy surface describing this reaction is much different from that proposed by Jones for the reaction of (η^5-Me_5C_5)(PMe_3)Rh with benzene. In the reaction of (η^5-Me_5C_5)(PMe_3)Rh with benzene, it has been suggested that the η^2-arene complex is an intermediate on the pathway leading to C–H bond activation. Indeed, the intermediate in the Rh system was shown to be ca. 20 kcal/mol less stable that (η^5-Me_5C_5)(PMe_3)Rh(C_6H_5)(H). In our case, however, the η^2-olefin complex is *more* stable than the C–H insertion product. This change in the relative stability of the η^2-complex could be caused either by the products being of much different stabilities or by different relative stabilities of the η^2-complexes. Thermodynamic studies conducted on the iridium system predict that the phenyl hydride and the vinyl hydride for a given system should be of comparable stability, indicating that the η^2-complex is responsible for the different ordering of stabilities. This is indeed reasonable, as one would predict that the loss of resonance energy during formation of an η^2-arene complex, as well as a larger steric demand, would tend to destabilize it relative to an η^2-olefin complex.

Because the ethylene π-complex is stable to the reaction conditions, we propose that the intermediate required by our isotope studies is a metastable species formed by weak coordination of one or more ethylene C–H bonds to the iridium center. For reasons of brevity, we refer to this species as a σ-complex (metal interacting through the σ-bonds of ethylene as opposed to the π-bond); analogous intramolecular species have been referred to as having "agostic" interactions.[34] There are a variety of possibilities for the structure of the σ-complex intermediate (Figure 10). We had hoped that experiments using the different d_2 ethylenes would exhibit different intramolecular isotope effects which might have led us to favor one of these intermediates. For example, if an intermediate of type **A** (Figure 10), formed by reaction with ethylene-*1,1-*d_2, could only insert into the two C–H bonds near the metal center, we would anticipate an isotope effect different from that found for *cis*-ethylene-*1,2-*d_2. Furthermore, if in this intermediate the iridium center were not able to insert into the distant C–H bonds, the isotope effect observed would be the same as that seen for the *intermolecular* competition experiment (no competition is present in the second step). A similar situation exists for intermediates of type **B** when the ethylene used is *cis*-ethylene-*1,2-*d_2. Our equivalent intramolecular isotope effects, which are different from the intermolecular effect, indicate that our intermediate (or rapidly equilibrating) set of intermediates must be able to choose between all four C–H bonds.

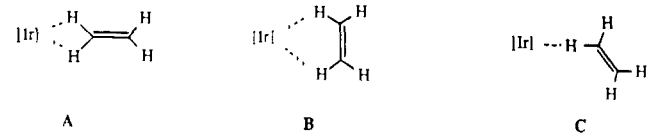

Figure 10. Possible structures for the intermediate on the pathway leading to C–H bond insertion.

Scheme XIII

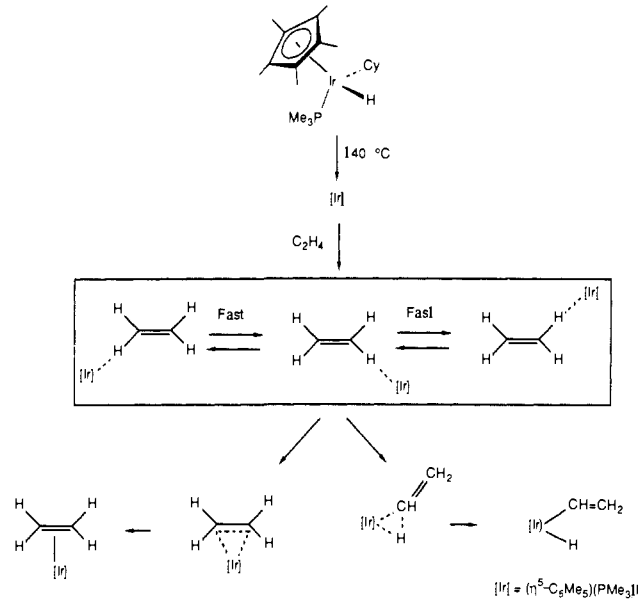

Because of these considerations, the fact that the different isomers of ethylene-d_2 give essentially identical ratios of C–H to C–D insertion products (i.e., identical intramolecular isotope effects) is a most surprising and perplexing result. The only way to account for this observation is to assume that once formed, the metal center in the σ-complex intermediate has access to *all* the C–H and C–D bonds in the molecule. Since it is difficult to conceive of an intermediate (other than the π-complex, which is ruled out) with an appropriate symmetry high enough to ensure this, we are forced to conclude that several isomeric σ-complexes, such as those illustrated in the box in Scheme XIII, equilibrate rapidly with one another on a time scale rapid with respect to conversion to the final products **1** and **2**.[35]

σ-Complex intermediates such as those discussed here have been proposed earlier. Upon co-condensation of iron atoms and ethylene in a matrix, ethylene–iron adducts are formed which upon irradiation isomerize to (H)Fe(HC=CH_2).[36] On the basis of infrared

(34) A referee has questioned our use of the term "σ-complex" to describe such an intermediate, because the primary orbital interactions between the C–H bonds and metal center in structures such as **A** or **B** in Figure 10 can be thought of as having π rather than σ *symmetry*. Therefore, we emphasize that our use of the term σ-complex is based on the historical definition of π-complex, which was *not* coined as a result of the symmetry of the interaction, but rather to indicate that an alkene was involved as one of the partners in the complex. For example, one of the earliest postulated π-complexes, formed from the symmetrical interaction of a proton with the π-electrons of ethylene, does not have π-symmetry. The alternative term "agostic", defined as "to clasp or hold to oneself" (see ref 34a), seems to be clearly limited to intramolecular C–H/metal interactions (hence it has not been adopted to describe the recently discovered metal–H_2 complexes; see ref 34b). Therefore, in analogy to the definition of "π-complex" outlined above, it seems convenient to utilize the simple phrase "σ-complex" as a general term to refer to a species formed by interaction between the σ-electrons of a C–H bond (or, for that matter, any other type of σ-bond) with an empty orbital on an associated metal or other electrophile, regardless of the symmetry of the orbital interaction involved in that complex. (a) Brookhart, M.; Green, M. L. H. *J. Organomet. Chem.* **1983**, *250*, 395. (b) Kubas, G. J.; Ryan, R. R.; Swanson, B. I.; Vergamini, P. J.; Wasserman, H. J. *J. Am. Chem. Soc.* **1984**, *106*, 451.

(35) An interesting alternative possibility is the competitive formation of an "end-on" and "side-on" intermediates **A** and **B** in Figure 10; we cannot conclusively rule this out. We are grateful to Drs. John Groves and Jay Labinger for suggestion and discussion of this possibility.

evidence which indicated a weakening of a C–H stretching vibration, σ-complexed species were proposed. In addition, ab initio calculations in which the energy surface for $M(CH_3)(H) \rightarrow M + CH_4$ (M = Pd, Pt) was explored have shown an energy minimum corresponding to methane σ-complexes in which more than one C–H bond simultaneously interacts with the metal.[37]

Conclusions

These results constitute one of the first direct observations of insertion into the C–H bonds of unactivated olefins. Along with more recent studies of similar systems, our experiments show that at least in cases where the vinyl hydride is stable, it is the predominant, if not the exclusive, kinetic product. Furthermore, in all of the studies the olefin π-complex was found to be the thermodynamically preferred product. This suggests that vinyl hydrides may not be as predominant in the chemical literature for thermodynamic reasons, and that there may be examples where vinyl hydrides are kinetically important intermediates on the pathway leading to formation of olefin complexes. This may be especially important for the later transition elements that are known to be capable of oxidative addition.

It is also important to consider the relative barriers to C–H activation and π-complex formation. In all of the cases where intermolecular insertion into the C–H bonds of unactivated alkenes has been observed, the metal-containing species is a highly unstable, unsaturated metal fragment. In our system, for example, $(\eta^5\text{-}Me_5C_5)(PMe_3)Ir$, formed by reductive elimination of cyclohexane from $(\eta^5\text{-}Me_5C_5)(PMe_3)Ir(C_6H_{11})(H)$, cannot exist in the square-planar geometry normally preferred by Ir(I) due to restrictions imposed by the cyclopentadienyl ligand. The high energy of intermediates such as these results in a lowering of the barrier to C–H insertion, and it is also one of the reasons they form very strong M–C and M–H bonds. It is not clear, however, that more stable organometallic fragments, many of which form π-complexes, are capable of overcoming the barrier to C–H insertion. Thus, while it is tempting to speculate that many reactions between olefins and transition-metal complexes go via metal–vinyl species which rearrange to the more stable η^2-olefin complexes, olefin complex formation may be kinetically favored relative to C–H insertion for less reactive metal complexes.

The thermodynamic stability of olefin complexes has been shown to be particularly sensitive to steric effects.[38] The kinetic barriers for formation of these complexes are also sensitive to steric effects. Of the complexes known to be capable of both CH insertion and π-complex formation, $(\eta^5\text{-}C_5Me_5)(PMe_3)$ is the least sterically demanding of the three, and gives rise to the largest amount of olefin complex formation.[12,13] Extended Hückel calculations of the reaction of $(\eta^5\text{-}Me_5C_5)(PMe_3)Ir$ with ethylene predict that while the enthalpic barrier to formation of $(\eta^5\text{-}Me_5C_5)(PMe_3)Ir(H_2C{=}CH_2)$ may be very small, its rate of formation is likely to be strongly influenced by the sterically demanding pentamethylcyclopentadienyl ligand.[39] This suggests that metal–vinyl species may be especially important intermediates when the metal is in a sterically demanding environment.

While there is good evidence that many catalytic processes proceed via metal–olefin π-complexes, evidence for metal–vinyl intermediates in some processes is beginning to accumulate. Faller and Felkin[40] have recently provided evidence for the intermediacy of metal–vinyl intermediates in H/D exchange reactions between benzene-d_6 and 3,3-dimethylbutene catalyzed by $[(i\text{-}Pr_3P)_2IrH_5]$. In these experiments deuterium is exchanged into the the position trans to the *tert*-butyl group ten times faster than into the geminal position. This is not consistent with the traditional mechanism involving addition/elimination of the olefin, where there would be expected to be deuterium in both terminal positions and in the geminal position. The selectivity observed suggests a different mechanism, perhaps vinylic C–H activation, similar to the mechanisms proposed for arene H/D exchange.

Kinetic evidence supports the intermediacy of metal–vinyl species in the formation of molybdenum metathesis catalysts.[41] The initial rates of propene metathesis were shown to be particularly sensitive to deuterium in the terminal position of the olefin. No isotope effect was observed for the rate of propene metathesis when propene was admitted onto a surface on which the carbene catalyst had earlier been formed. This was judged to be most consistent with a rate-determining formation of a metal vinyl hydride which then undergoes a hydrogen shift to give the species believed to be responsible for metathesis. Similarly, there are other catalytic reactions for which one may wish to consider metal–vinyl complexes as viable intermediates.[42] Recently, studies of the interaction of olefins with single metal crystals have shown that metal–vinyl species may be formed there as well.[43]

Finally, our most perplexing result is the essentially identical intramolecular isotope effects measured for insertion of $(\eta^5\text{-}C_5Me_5)(PMe_3)Ir$ into the C–H and C–D bonds of *cis*- and *trans*-ethylene-*1,2-d*$_2$ and ethylene-*1,1-d*$_2$. This requires an intermediate which, on the average, has access to all the hydrogen and deuterium atoms in each isomer of the C–**H**-coordinated ethylene on a time scale rapid with respect to further reaction of the intermediate. We have suggested the rapidly equilibrating σ-complexes illustrated in Scheme XIII to account for this result. However, it seems surprising to us that isomerization of this species should be so facile compared with C–H insertion and π-complex formation. We therefore feel this postulate should be considered a working hypothesis and plan to seek its confirmation by further experimentation.

Experimental Section

General. All manipulations were carried out under argon or nitrogen with standard Schlenk or vacuum line techniques, or under a nitrogen atmosphere in a Vacuum Atmospheres 553-2 Dri-lab equipped with an MO-40-1(2)Dri-train, unless otherwise stated. ^1H NMR spectra were obtained on a 300-MHz spectrophotometer constructed using a Cryomagnet Systems 300/50 7.05 T magnet and a Nicolet 1280 computer by Rudi Nunlist of the UCB NMR Facility. ^{13}C NMR and ^{31}P NMR spectra were obtained on the same instrument operating at 74.4 and 121.5 MHz, respectively. ^2H NMR spectra were obtained on a Bruker AM-500 spectrophotometer operating at 76.77 MHz. ^1H, ^2H, and ^{13}C chemical shifts were referenced to the chemical shift of the solvent used as found in tables distributed by MSD Isotopes and are reported in parts per million downfield from tetramethylsilane. ^{31}P NMR shifts were referenced to an external standard of 85% H_3PO_4 and are reported in parts per million downfield from H_3PO_4. All coupling constants are reported in hertz. Infrared spectra were recorded on a Perkin-Elmer Model 283 grating spectrophotometer, or on a Perkin-Elmer Model 1550 Fourier transform spectrophotometer. Melting points were determined in sealed capillaries on a Thomas-Hoover melting point apparatus and are uncorrected. Elemental analyses were performed in the UCB elemental analysis facility. Mass spectroscopic analyses were obtained on an AEI MS-1 spectrophotometer interfaced with a Finnigan 2300 data system.

Pentane, hexane, and cyclohexane were spectral grade and were distilled from $LiAlH_4$. THF, toluene, and benzene were spectral grade and were distilled from Na/benzophenone. Ether was distilled from Na/benzophenone. Sodium borohydride and sodium borodeuteride (98% D) were purchased from Alpha and Aldrich Chemical Companies, respectively. Vinylmagnesium bromide was purchased as a 1.0 M solution in THF from the Aldrich Chemical Co. $(\eta^5\text{-}Me_5C_5)(PMe_3)Ir(H)_2$,[3a] $(\eta^5\text{-}Me_5C_5)(PMe_3)Ir(Cl)_2$,[44] and $(\eta^5\text{-}Me_5C_5)(PMe_3)Ir(C_6H_{11})(H)$[6] were

(36) Kafafi, Z. H.; Hauge, R. H.; Margrave, J. L. *J. Am. Chem. Soc.* **1985**, *107*, 7550.
(37) (a) Low, J. J.; Goddard, W. A. *J. Am. Chem. Soc.* **1984**, *106*, 8321. (b) Anderson, A. B.; Baldwin, S. *Organometallics* **1987**, *6*, 1621.
(38) (a) Herberhold, M. *Metal π-Complexes*; Elsevier: New York, 1974; Vol. 2. (b) Collman, J. P.; Hegedus, L. S.; Norton, J. R.; Finke, R. G. *Principles and Applications of Organotransition Metal Chemistry*; University Science Books: Mill Valley, CA, 1987; Chapter 3.
(39) Silvestre, J.; Calhorda, M. J.; Hoffman, R.; Stoutland, P. O.; Bergman, R. G. *Organometallics* **1986**, *5*, 1841.
(40) Faller, J. W.; Felkin, H. *Organometallics* **1985**, *4*, 1488.
(41) Iwasawa, Y.; Hamamura, H. *J. Chem. Soc., Chem. Commun.* **1983**, 130.
(42) (a) Pez, G. P. *J. Chem. Soc., Chem. Commun.* **1977**, 560. (b) Baudry, D.; Cormier, J.-M.; Ephritikhine, M.; Felkin, H. *J. Organomet. Chem.* **1984**, *277*, 99. (c) Green, M. L. H.; Knight, J. *J. Chem. Soc., Dalton Trans.* **1974**, 311. (d) Hudson, B.; Webster, D. E.; Wells, P. B. *J. Chem. Soc., Dalton Trans.* **1972**, 1204.
(43) Lehwald, S.; Ibach, H. *Surf. Sci.* **1979**, *89*, 425.

prepared according to published procedures; the latter complex was purified by low-temperature chromatography (vide post). PMe_3 was purchased from Strem Chemicals, dried over a sodium mirror and then vacuum transferred.

Ethylene used was CP grade and was transferred to a glass vessel fitted with a Kontes Teflon vacuum stopcock (No. 826500) where it was subjected to several freeze–pump–thaw cycles to remove any noncondensible gases. Deuteriated ethylenes were purchased in glass vessels from MSD Isotopes or from CIL, fitted with Teflon vacuum stopcocks and thoroughly degassed. The identities of ethylene-h_4 and ethylene-d_4 were confirmed by mass spectroscopy. The identities of ethylene-*1,1*-d_2, *cis*-ethylene-*1,2*-d_2, and *trans*-ethylene-*1,2*-d_2 were confirmed by infrared spectroscopy and were all >98% pure.[33] Gas quantities were measured by using known-volume bulbs and an MKS Baratron gauge to measure the pressure. The ideal gas law was used to determine the number of moles of gas present.

Benzene-d_6 was dried over Na/benzophenone. Cyclohexane-d_{12} was washed with a 2:1 mixture of HNO_3/H_2SO_4 to remove traces of benzene-d_6 and then washed with 25% NaOH and water. It was predried over $MgSO_4$, stirred over sodium/potassium alloy, and vacuum transferred into a glass vessel fitted with a Teflon vacuum stopcock.

All kinetics and reactions performed over 130 °C were done in a factory calibrated Neslab EX-250HT high-temperature bath accurate to 0.03 °C and filled with Dow Corning 210H fluid. Photolyses were performed with use of a 450 W Conrad-Hanovia medium pressure mercury lamp in an Ace 7874B-38 immersion well. The immersion well was placed into a dewar filled with water cooled to 5–10 °C by a recirculating bath. The sample was typically irradiated in a Pyrex NMR tube 2 in. from the light source.

The columns used in our laboratory for low-temperature chromatography consist of a vacuum jacketed middle jacket which has a solvent reservoir at the top. Between the inner tube and the vacuum jacket is a space with an inlet at the top and at the bottom. The top of the column has a 24/40 female joint leading into the column, as well as an inlet for gas which is fitted with a Kontes 4 mm Teflon stopcock (No. K-826500). The bottom of the column is also equipped with a vacuum stopcock which leads to a luer tip for connection to a syringe needle. The column is cooled by bubbling gaseous N_2 through a dewar of liquid N_2 and then through the middle jacket of the column. The temperature may be regulated by changing the rate of N_2 flow through the column. We have measured the temperature by inserting a thermocouple into the column and have found that temperatures of −80 to −100 °C are easily attainable. The chromatography is performed under air-free conditions by using Schlenk techniques, with detection by an MPLC UV detector (Altex Model 153 fitted with a preparatory cell).

Silica gel (SiO_2) was purchased from EM Reagents and was dried under vacuum at ca. 200 °C overnight. Alumina (Al_2O_3) was purchased from MCB Reagents and was deactivated to the appropriate grade by the addition of water as stated in *The Chemist's Companion*.

Thermolysis of (η^5-Me_5C_5)(PMe_3)Ir(C_6H_{11})(H) in the Presence of $H_2C{=}CH_2$. In the drybox an NMR tube was charged with 10.0 mg (0.025 mmol) of the cyclohexyl hydride complex (η^5-Me_5C_5)(PMe_3)Ir(C_6H_{11})(H) in 0.6 mL of C_6D_{12}. The NMR tube was fitted with a stopcock having a Cajon Ultra-Torr adapter and the apparatus attached to a vacuum line. On the vacuum line 2.97 mmol of $H_2C{=}CH_2$ was condensed into the tube, after which it was sealed in vacuo. The tube was heated at 130 °C. After ca. 3 h both (η^5-Me_5C_5)(PMe_3)Ir(HC=CH_2)(H) (**1**) and (η^5-Me_5C_5)(PMe_3)Ir($H_2C{=}CH_2$) (**2**) had been formed, as determined by comparison of the ^1H NMR spectrum with NMR data obtained on samples of these compounds prepared by independent synthesis (see below). The total yield of the two products, as estimated by integration vs the residual proton peak in the solvent, was >90%. The vinyl hydride to ethylene complex ratio was 64:36, and this ratio was unchanged after 79 h. Further experimentation revealed that both products were completely stable to the reaction conditions.

Thermolysis of (η^5-Me_5C_5)(PMe_3)Ir(HC=CH_2)(H). In a typical experiment 11.5 mg (0.0266 mmol) of (η^5-Me_5C_5)(PMe_3)Ir(C_6H_{11})(H) and 2.7 μL of hexamethyldisiloxane (0.013 mmol) as an internal standard were dissolved in 0.433 g (0.485 mL) of C_6D_{12} in the drybox. This was put into a Wilmad 504PP NMR tube and sealed in a vacuo. The tube was heated at 200.0 °C. The extent of reaction was monitored by comparison of the signals from the cyclopentadienyl ligand or from the PMe_3 ligand with those of the internal standard. During the reaction, it was clear that some (<5%) of the iridium-containing material was decomposing to NMR-silent material. To minimize the effect of this on the kinetics, we estimated the concentration of the product at $t = \infty$. This was done by an iterative procedure on an IBM-PC whereby C_∞ was varied until the best correlation coefficient was found for a plot of $-\ln(C_\infty - C_t)$ vs time. The rates reported are those determined from the slope of the line resulting from a plot of $-\ln(C_\infty - C_t)$ vs time. The slope of the line found in this manner led to a rate constant of 3.49×10^{-3} s^{-1} for this particular experiment ($r = 0.998$). A similar procedure was used for the other temperatures.

(44) Kang, J. W.; Moseley, K.; Maitlis, P. M. *J. Am. Chem. Soc.* **1969**, *91*, 5970.

Table 6. Intermolecular isotope effect data. Amounts of products are relative to [Ir](C_6H_5)(H).

Exp. #	Gas	[Ir](C_6H_5)(H)	1	2	k_H/k_D(1)	k_H/k_D(2)
1	$H_2C{=}CH_2$	(1.00)	0.79	0.43	1.55	0.84
	$D_2C{=}CD_2$	(1.00)	0.51	0.51		
2	$H_2C{=}CH_2$	(1.00)	0.79	0.39	1.46	0.80
	$D_2C{=}CD_2$	(1.00)	0.54	0.49		
3	$H_2C{=}CH_2$	(1.00)	0.77	0.41	1.45	0.81
	$D_2C{=}CD_2$	(1.00)	0.53	0.50		

We have found it difficult to isolate analytically pure **2**. In contrast to the iridium alkyl hydride complexes, it moves only slowly on chromatography supports and elutes impure. In cases where the conversion of **1** to **2** is particularly clean, we have been able to isolate analytically pure (η^5-Me_5C_5)(PMe_3)Ir($H_2C{=}CH_2$) by high-vacuum sublimation at slightly above ambient temperature, with the product being isolated as an amorphous solid. ^1H NMR (C_6D_6) δ 1.86 (d, η^5-Me_5C_5, J_{P-H} = 1.5 Hz), 1.01 (d, PMe_3, J_{P-H} = 9.0 Hz), 1.13, 1.27 (m, $H_2C{=}CH_2$); ^{13}C NMR (C_6D_6) δ 10.29 (q, η^5-Me_5C_5, J_{C-H} = 126.1 Hz), 90.19 (s, η^5-Me_5C_5), 10.55 (dd, $H_2C{=}CH_2$, $J_{C-H1} = J_{C-H2}$ = 150.6 Hz), 16.93 (q, PMe_3, J_{P-C} = 33.9 Hz, J_{C-H} = 128.3 Hz); IR (C_6D_6) 2960 (s), 2900 (s), 1360 (s), 940 (s); MS (70 eV) 432 (M^+), 404 ($M^+ - C_2H_4$). Anal. Calcd: C, 41.75; H, 6.54. Found: C, 41.77; H, 6.55.

Photolysis of (η^5-Me_5C_5)(PMe_3)Ir($H_2C{=}CH_2$). In the drybox an NMR tube was charged with 5.3 mg (0.0123 mmol) of (η^5-Me_5C_5)(PMe_3)Ir($H_2C{=}CH_2$) in 1.0 mL of C_6D_{12}. This was irradiated and monitored by ^1H NMR. After 1 h the reaction mixture was >95% (η^5-Me_5C_5)(PMe_3)Ir(HC=CH_2)(H).

Intermolecular Isotope Effects. A typical experiment was done in the following way. In the drybox a solution of 34.4 mg (0.0706 mmol) of (η^5-Me_5C_5)(PMe_3)Ir(C_6H_{11})(H) and 60 μL (0.671 mmol) of C_6H_6 (as measured by syringe) was dissolved in 1.30 g (1.45 mL) of cyclohexane-d_{12}. This was split equally among three Wilmand 504PP NMR tubes, two of which were used for this experiment. The NMR tubes were subsequently attached to a vacuum line with Cajon Ultra-Torr adapters. PMe_3 (17.2 Torr in 5.72 mL) and $H_2C{=}CH_2$ (150.0 Torr in 141.2 mL; 1.14 mmol) were vacuum transferred into one tube. PMe_3 (16.8 Torr in 5.72 mL; 0.005 mmol) and $D_2C{=}CD_2$ (149.8 Torr in 141.2 mL; 1.14 mmol) were transferred into the other tube. Both tubes were then sealed at a length of ca. 25 ± 0.3 cm. These were then heated, side-by-side, at 145.5 °C for 15.5 h. ^1H NMR analysis revealed the reaction to be complete. The relative amounts of (η^5-Me_5C_5)(PMe_3)Ir(C_6H_5)(H), (η^5-Me_5C_5)(PMe_3)Ir(HC=CH_2)(H), and (η^5-Me_5C_5)(PMe_3)Ir($H_2C{=}CH_2$), determined with ^{31}P NMR with pulse delays of at least $10T_1$, were determined to be 1.00:0.79:0.39. In the second tube, the relative amounts of (η^5-Me_5C_5)(PMe_3)Ir(C_6H_5)(H), (η^5-Me_5C_5)(PMe_3)Ir(DC=CD_2)(D), and (η^5-Me_5C_5)(PMe_3)Ir($D_2C{=}CD_2$) were found to be 1.00:0.54:0.49. By comparing the amount of (η^5-Me_5C_5)(PMe_3)Ir(HC=CH_2)(H) to (η^5-Me_5C_5)(PMe_3)Ir(DC=CD_2)(D) (both normalized to the amount of (η^5-Me_5C_5)(PMe_3)Ir(C_6H_5)(H) formed), one can determine the intermolecular isotope effect: k_H/k_D = 1.46. Similarly for the π-complex formation k_H/k_D = 0.80. This experiment was repeated 3 times, reducing the uncertainty in each of these isotope effects. The final values are k_H/k_D(insertion) = 1.49 ± 0.08 and k_H/k_D(π-complex formation) = 0.82 ± 0.05. In Table 6 are summarized the data from three experiments.

Intramolecular Isotope Effects. In a typical experiment, 10.0 mg (0.0205 mmol) of (η^5-Me_5C_5)(PMe_3)Ir(C_6H_{11})(H) and 20 μL of benzene were dissolved in 0.435 g (0.487 mL) of C_6H_{12} in a Wilmad 504PP NMR tube. The NMR tube was attached to a Kontes Teflon vacuum stopcock with a Cajon Ultra-Torr fitting (SS-6-UT-6-4) and evacuated on a vacuum line. *cis*-Ethylene-*1,2*-d_2 (148 Torr in 141.2 mL) and PMe_3 (18.7 Torr in 5.72 mL) were then vacuum transferred into the NMR tube, and the tube was flame sealed. The tube was heated for 20 h at 145.0 °C. Using an apparatus which allows an NMR tube to be broken open under vacuum, we froze the solution at −196 °C and broke open the tube. It was allowed to warm to −78 °C and the ethylene remaining was collected at −196 °C in another vessel. The NMR tube was then resealed in vacuo at −196 °C. Mass spectral analysis of the ethylene removed showed that it was >96% ethylene-d_2. The ^2H NMR of the organometallic products, using sufficiently long relaxation times for accurate integrations (5 s), showed that insertion into a C–H bond in ethylene was favored over insertion into a C–D bond by a factor of 1.20. This was determined by comparing the amount of deuterium in the

hydride position versus that in the β-position on the vinyl group trans to the metal, which was equal to the ratio found by comparing the amount of deuterium in the α-positions on the vinyl group to that in the β-position cis to the metal. Experiments with all of the d_2 ethylenes showed no significant difference in the values found. The values from five experiments were averaged, reducing the error from a single measurement, k_H/k_D(intramolecular insertion effect) = 1.18 ± 0.03. A table showing the isotope effects found for each experiment is given in the text.

Relative Solubilities of Ethylene and Ethylene-d_4. The relative solubilities were measured by using the apparatus shown in Figure 8. It consists of a stainless steel bomb (fitted with a long neck so as to prevent the Nupro valve from freezing during the freeze–pump–thaw cycles) attached to a stainless steel pipe with a Nupro bellows valve (No. SS-2H2). The top of the stainless steel tube is fitted with another Nupro valve which has a fitting to allow connection to a vacuum line. The volume of the lower bomb was 11.2 mL, and the volume between the two valves was approximately 30 mL.

A typical measurement was performed as follows. The stainless steel bomb was removed from the apparatus and filled with 7.30 g (9.37 mL) of cyclohexane. This was then re-attached to the apparatus. On a vacuum line, this was subjected to 7 freeze–pump–thaw cycles. Completely degassed ethylene was expanded into a 508.5-mL bulb at a pressure of 136 Torr (3.734 mmol) and was then condensed into the apparatus. The pressure in the vacuum line decreased steadily until it was less than 0.1 Torr, at which time the upper valve of the apparatus was closed. After 2.5 h at room temperature the apparatus had equilibrated, and the lower valve was closed. The gases is the upper section of the apparatus were passed through two −78 °C traps to freeze out any cyclohexane and then measured with a Toepler pump. The amount of gas collected increased sharply for the first 15 min and then remained constant for 2 h, at which time the experiment was stopped. The amount of gas measured was converted to moles by using the ideal gas law; in this case 2.89 mmol (31.3 mm in 169 mL) was collected. Subtraction of the amount above the solution from the total amount of ethylene used resulted in determination of the amount in solution (3.73 − 2.89 = 0.84 mmol).

The solubilities of ethylene and ethylene-d_4 were each measured twice. The two experiments with ethylene showed 2.89 and 2.83 mmol of ethylene above the solution, respectively, whereas the two experiments with ethylene-d_4 showed 2.81 and 2.74 mmol above the solution, respectively.

$(\eta^5\text{-}Me_5C_5)(PMe_3)Ir(HC{=}CH_2)(Br)$. In the drybox, 1.044 g (2.20 mmol) of $(\eta^5\text{-}Me_5C_5)(PMe_3)IrCl_2$ was dissolved in 65 mL of THF. With stirring, 2.6 mL of a 1.0 M solution (2.6 mmol) of $H_2C{=}CHMgBr$ in THF was added. This was stirred at the drybox temperature (15–20 °C) for 12 h during which time the solution changed from orange to yellow. This was then passed through a short pad of SiO_2. Further purification was effected on the benchtop (in air). Chromatography with a 3.5 × 20 cm column of SiO_2 with 30% ether/hexane as the eluent allowed us to isolate the product which eluted as a broad yellow band, occasionally contaminated with what is thought to be $(\eta^5\text{-}Me_5C_5)(PMe_3)Ir(HC{=}CH_2)(Cl)$ if an insufficient amount of $H_2C{=}CHMgBr$ used: yield 757 mg (67.4%). ^1H NMR (C_6D_6) δ 1.26 (d, PMe_3, $J_{P\text{-}H}$ = 10.5 Hz), 1.51 (d, $\eta^5\text{-}Me_5C_5$, $J_{P\text{-}H}$ = 1.9 Hz), 5.39, 6.68 (m, $-CHCH_2$), 9.40 (ddd, $-CHCH_2$, $J_{P\text{-}H}$ = 1.2 Hz, $J_{H\text{-}H(cis)}$ = 10.2 Hz, $J_{H\text{-}H(trans)}$ = 17.3 Hz); ^{13}C NMR (C_6D_6) δ 9.18 (q, $\eta^5\text{-}Me_5C_5$, $J_{C\text{-}H}$ = 128.2 Hz), 14.58 (dq, PMe_3, $J_{P\text{-}C}$ = 40.1 Hz, $J_{C\text{-}H}$ = 129.4 Hz), 92.44 (s, $\eta^5\text{-}Me_5C_5$), 118.71 (dt, $-CHCH_2$, $J_{P\text{-}C}$ = 4.8 Hz, $J_{C\text{-}H}$ = 151.1 Hz), 142.52 (dd, $-CHCH_2$, $J_{P\text{-}C}$ = 17.5 Hz, $J_{C\text{-}H}$ = 144.6 Hz); IR (KBr) 1550 (m), 1415 (s), 1280 (s), 945 (s); MS (70 eV) 510 (M^+), 483 ($M^+ - C_2H_3$); mp 192–204 °C dec. Anal. Calcd: C, 35.29; H, 5.33. Found: C, 35.43; H, 5.27.

$(\eta^5\text{-}Me_5C_5)(PMe_3)Ir(HC{=}CH_2)(H)$. In a Schlenk flask, 214 mg (0.420 mmol) of $(\eta^5\text{-}Me_5C_5)(PMe_3)Ir(HC{=}CH_2)(Br)$ and 40.5 mg (1.07 mmol) of $NaBH_4$ were dissolved in 2-propanol. The solution was then degassed and put under argon. This was stirred for 6 h at 50 °C during which time the solution became nearly colorless. The solvent was removed in vacuo leaving a white solid. Chromatography at −80 °C under Ar with Al_2O_3 (III) and 5% ether/pentane was used to purify the product, which eluted near the solvent front. Yield: 150 mg (83%). Positive argon pressure was used to elute the product, as it isomerizes to $(\eta^5\text{-}Me_5C_5)(PMe_3)Ir(H_2C{=}CH_2)$ if left on the column for longer than ca. 5 min. Alternatively, the product may be taken up in pentane and filtered through Celite and then recrystallized from highly concentrated solutions of pentane or hexamethyldisiloxane. ^1H NMR (C_6D_6) δ 1.86 (dd, $\eta^5\text{-}Me_5C_5$, $J_{P\text{-}H}$ = 1.8 Hz, $J_{H\text{-}H}$ = 0.8 Hz), 1.24 (d, PMe_3, $J_{P\text{-}H}$ = 10.1 Hz), 5.75, 6.95 (m, $-CHCH_2$), 8.12 (ddd, $-CHCH_2$, $J_{P\text{-}H}$ = 3.3 Hz, $J_{H\text{-}H(cis)}$ = 10.2 Hz, $J_{H\text{-}H(trans)}$ = 17.5 Hz), −16.88 (d, −H, $J_{P\text{-}H}$ = 36.0 Hz); ^{13}C (C_6D_6) δ 10.27 (s, $\eta^5\text{-}Me_5C_5$), 18.82 (d, PMe_3, $J_{P\text{-}C}$ = 38.6 Hz), 92.50 (d, $\eta^5\text{-}Me_5C_5$, $J_{P\text{-}C}$ = 2.6 Hz), 123.78 (d, $-CHCH_2$, $J_{P\text{-}C}$ = 3.0 Hz), 129.18 (d, $-CHCH_2$, $J_{P\text{-}C}$ = 13.4 Hz); IR (KBr) 2903 (s), 2105 (s), 1553 (s), 953 (s), 940 (s); MS (70 eV) 432 (M^+), 404 ($M^+ - C_2H_4$); mp 65–68 °C. Anal. Calcd: C, 41.75; H, 6.54. Found: C, 41.65; H, 6.63.

Table 7. Crystal and Data Collection Parameters for 1.

Compound: $(\eta^5\text{-}Me_5C_5)(PMe_3)Ir(HC{=}CH_2)(H)$

(A) Crystal Parameters at −118±4 °C[a,b]

a = 10.5245(12) A	Space Group: $P2_1/n$
b = 12.7267(16) A	Formula Weight = 431.6 amu
c = 12.3606(18) A	Z = 4
β = 94.052(11) °	d_c = 1.74 g/cm^3
V = 1651.5(7) A^3	
μ (calc) = 81.3 cm^{-1}	

Size of crystal: 0.18 x 0.20 x 0.40 mm

(B) Data Measurement Parameters

radiation: Mo Kα (λ = 0.71073 A)
monochrometer: highly-oriented graphite (2θ = 12.2°)
detector: crystal scintillation counter, with PHA.
reflections measured: +h, +k, ±l
2θ range: 3° --> 55° Scan Type: θ - 2θ
scan width: Δθ = 0.55 + 0.347 tan(θ)
scan speed: 0.66 --> 6.7 (θ, °/min)
background: measured over 0.25(Δθ) added to each end of the scan.
aperture --> crystal = 173 mm vertical aperture = 3.0 mm
horizontal aperture = 2.0 + 1.0 tan(θ) mm (variable).
no. of reflections collected: 4143
no. of unique reflections: 3268
intensity standards: (474), (447), (635); measured every hour of x-ray exposure time. Over the data collection period no decrease in intensity was observed.
orientation: 3 reflections were checked after every 250 measurements. crystal orientation was redetermined if any of the reflections were offset from their predicted positions by more than 0.1°. Reorientation was performed one during data collection.

[a] Unit cell parameters and their esd's were derived by a least-squares fit to the setting angles of the unresolved Mo Kα components of 24 reflections with 2θ between 29° and 31°.
[b] The esd's of all parameters are given in parentheses, right-justified to the least significant digit(s) given.

Table 8. Positional Parameters and Their Estimated Standard Deviations.

atom	x	y	z	B(A)^2
IR	0.00156(1)	0.18211(1)	0.30935(1)	1.568(2)
P	0.0241(1)	0.00962(8)	0.28788(8)	2.01(2)
C1	-0.1724(3)	0.2269(3)	0.1988(3)	2.02(7)
C2	-0.2084(3)	0.2218(3)	0.3093(3)	1.97(6)
C3	-0.1364(4)	0.2996(3)	0.3702(3)	2.06(7)
C4	-0.0533(4)	0.3509(3)	0.3007(3)	2.03(7)
C5	-0.0790(4)	0.3066(3)	0.1931(3)	2.07(7)
C6	-0.2340(4)	0.1663(4)	0.1057(4)	3.21(9)
C7	-0.3160(4)	0.1592(4)	0.3489(4)	3.01(8)
C8	-0.1512(5)	0.3288(3)	0.4861(4)	3.16(9)
C9	0.0344(4)	0.4404(3)	0.3286(4)	3.09(9)
C10	-0.0211(5)	0.3432(4)	0.0933(3)	3.26(9)
C11	0.1817(4)	0.1940(3)	0.2566(4)	2.96(8)
C12	0.2943(5)	0.1868(4)	0.3057(5)	3.8(1)
C13	0.1484(5)	-0.0541(3)	0.3734(4)	3.18(9)
C14	0.0620(5)	-0.0305(4)	0.1527(3)	3.9(1)
C15	-0.1120(5)	-0.0725(3)	0.3119(4)	3.53(9)
H1	0.071(5)	0.158(4)	0.427(4)	5(1)*
H11	0.183(5)	0.200(4)	0.171(4)	5(1)*
H12A	0.366(5)	0.197(3)	0.263(4)	4(1)*
H12B	0.305(4)	0.168(3)	0.378(3)	2.4(9)*
H6A	-0.310(6)	0.194(4)	0.077(5)	6(2)*
H6B	-0.177(5)	0.139(4)	0.064(4)	5(1)*
H6C	-0.251(5)	0.090(4)	0.125(4)	4(1)*
H7A	-0.395(5)	0.197(4)	0.335(4)	4(1)*
H7B	-0.328(4)	0.106(3)	0.312(3)	3(1)*
H7C	-0.308(6)	0.135(5)	0.424(4)	6(1)*
H8A	-0.215(5)	0.387(4)	0.485(4)	4(1)*
H8B	-0.189(5)	0.275(4)	0.528(4)	5(1)*
H8C	-0.073(6)	0.353(5)	0.519(5)	6(1)*
H9A	-0.009(4)	0.491(4)	0.314(3)	5(1)*
H9B	0.075(4)	0.439(3)	0.400(3)	3(1)*
H9C	0.103(4)	0.444(3)	0.281(3)	2.4(9)*
H10A	-0.061(5)	0.407(4)	0.061(4)	4(1)*
H10B	0.068(5)	0.372(4)	0.110(4)	4(1)*
H10C	-0.034(5)	0.298(4)	0.035(4)	4(1)*
H13A	0.160(4)	-0.117(3)	0.353(3)	2.3(9)*
H13B	0.231(5)	-0.009(4)	0.368(4)	5(1)*
H13C	0.118(6)	-0.048(4)	0.439(4)	6(1)*
H14A	0.073(7)	-0.088(6)	0.150(5)	9(2)*
H14B	-0.007(5)	-0.008(4)	0.109(4)	5(1)*
H14C	0.147(5)	0.021(4)	0.129(4)	5(1)*
H15A	-0.090(5)	-0.135(4)	0.306(4)	4(1)*
H15B	-0.139(4)	-0.057(3)	0.381(3)	4(1)*
H15C	-0.183(5)	-0.050(4)	0.261(4)	4(1)*

* Atoms refined with isotropic thermal parameters.

X-ray Data Collection, Structure Determination, and Refinement for $(\eta^5\text{-}Me_5C_5)(PMe_3)Ir(HC{=}CH_2)(H)$. Clear, yellow needle-like crystals were obtained by slow crystallization from hexamethyldisiloxane. Fragments cleaved from some of these crystals were mounted in capillaries in the air, flushed with dry nitrogen, and then flame sealed. Precession photographs indicated monoclinic Laue symmetry and yielded preliminary cell dimensions. Systematic absences were consistent only with space group $P2_1/n$.

The crystal used for data collection was transferred to our Enraf-Nonius CAD-4 diffractometer and centered in the beam. It was cooled to −118 °C by a gaseous nitrogen flow apparatus, and the temperature

was monitored by an in-stream thermocouple which had been previously calibrated against a second thermocouple in the sample position. Automatic peak search and indexing procedures yielded the monoclinic reduced primitive cell. The final cell parameters and specific collection parameters are given in Table 7.

The 4143 raw intensity data were converted to structure factor amplitudes and their esd's by correction for scan speed, background, and Lorentz and polarization effects. No correction for crystal decomposition was necessary. Inspection of the azimuthal scan data showed a variation $I_{min}/I_{max} = 0.75$ for the average curve. An empirical correction for absorption, based on the azimuthal scan data, was applied to the intensities since it was not possible to accurately measure the sample crystal. Removal of systematically absent and redundant data left 3775 unique data.

The structure was solved by Patterson methods and refined via standard least-squares and Fourier techniques. In a difference Fourier map calculated following refinement of all non-hydrogen atoms with anisotropic thermal parameters, peaks corresponding to the expected positions of most of the hydrogen atoms were found. A difference Fourier map calculated after inclusion of all other hydrogen atoms clearly showed the position of the hydride ligand attached to the metal. All hydrogen atoms were then allowed to refine with isotropic thermal parameters. A secondary extinction parameter was refined in the final cycles of least-squares. The final residuals for 267 variables refined against the 3100 data for which $F^2 > 3|F^2|$ were $R = 2.04\%$, $wR = 2.53\%$, and GOF = 1.356. The R value for all 3775 data was 3.49%.

The quantity minimized by the least-squares program was $w(|F_o| - |F_c|)^2$ where w is the weight of a given observation. The p factor, used to reduce the weight of intense reflections, was set to 0.025 in the last cycles of the refinement. The analytical forms of the scattering factor tables of the neutral atoms were used, and all non-hydrogen scattering factors were corrected for both the real and imaginary components of anomalous dispersion.

Inspection of the residuals ordered in ranges of sin $(\theta)/\lambda$, $|F_o|$, and parity and value of the individual indices showed no unusual features or trends. The largest peak in the final difference Fourier map had an electron density of 2.14 $e^-/Å^3$ and was located only 0.74 Å from the iridium atom. All other peaks in the final difference Fourier map had densities of less than 1 $e^-/Å^3$. The positional parameters of the atoms and the estimated standard deviations are given in Table 8. Structure factor amplitudes were provided as supplementary material in the preliminary communication.[4]

Acknowledgment. This work was carried out under the auspices of a collaborative Lawrence Berkeley Laboratory/Industrial research project supported jointly by the Chevron Research Company, Richmond, CA, and the Director, Office of Energy Research, Office of Basic Energy Sciences, Chemical Sciences Division of the U.S. Department of Energy under Contract No. DE-AC03-76SF00098. We are also grateful for helpful discussions with Drs. J. A. Labinger and J. T. Groves and for a loan of iridium chloride from the Johnson-Matthey Corp. We thank Sue Rossi for Figure 7.

Synthesis and Reactions of Dinuclear Palladium Complexes Containing Methyls and Hydride on Adjacent Palladium Centers: Reductive Elimination and Carbonylation Reactions

S. J. Young, B. Kellenberger, Joseph H. Reibenspies, S. E. Himmel, M. Manning, Oren P. Anderson, and J. K. Stille*

Contribution from the Department of Chemistry, Colorado State University, Fort Collins, Colorado 80523. *Received December 4, 1987*

Abstract: The transmetalation reaction of trimethylaluminum with the palladium chloride dimer $Pd_2Cl_2(\mu\text{-dppm})_2$ (**1**) (dppm = bis(diphenylphosphino)methane) at −78 °C gave an intermediate, $Pd_2ClMe(\mu\text{-dppm})_2$ (**2**), which disproportionated at ~10 °C to yield the trans-face-to-face palladium dimer $Pd_2Cl_2Me_2(\mu\text{-dppm})_2$ (**3**) and a palladium dimer $Pd_2Cl_2(\mu\text{-}CH_2)(\mu\text{-dppm})_2$ (**5**). The use of excess trimethylaluminum at −40 °C gave the dimethyl complex, $Pd_2Me_2(\mu\text{-dppm})_2$ (**7**). When **2** and **7** were protonated, a stable A-frame chloro-bridged dimer $[Pd_2HMe(\mu\text{-Cl})(\mu\text{-dppm})_2]^+$ (**6**) and a hydride-bridged dimer $[Pd_2Me_2(\mu\text{-H})(\mu\text{-dppm})_2]^+$ (**8**) were obtained. Warming **6** in solution to ambient temperature caused the reductive elimination of methane; **8** lost methane and ethane at ambient temperatures. Both reductive eliminations were strictly intramolecular as determined by crossover experiments. The reaction of **6** with CO (1 atm) at −20 °C first gave a carbonyl-bridged complex $[Pd_2Me(H)(\mu\text{-Cl})(\mu\text{-CO})(\mu\text{-dppm})_2]^+$ (**10**) that rearranged to the acyl complex $[Pd_2H(COCH_3)(\mu\text{-Cl})(\mu\text{-dppm})]^+$ (**11**) and then on warming eliminated acetaldehyde. The carbonylation of **8** (1 atm) proceeded stepwise to give first the mono- and then the diacyl complexes. The diacyl complex $[Pd_2(COCH_3)_2(\mu\text{-H})(dppm)_2]^+$ (**13**) underwent the reductive elimination of acetaldehyde at ambient temperatures.

Metal dimers are the simplest conceptual models of metal surfaces in catalysts but have the advantage that because of their relatively good solubility, a study of their reactions is comparitively simple.[1] The mechanistic features of the reactions of organic fragments on metal dimers or clusters can be established more readily than those of reactions taking place on surfaces, at least with the present state of the available methods and physical characterization techniques.[2]

There are a number of reactions of metal dimers and clusters that are unique in their mode of transformation and bonding as compared to homogeneous catalysts containing a single metal atom.[1,3] It has been suggested that the lack of reactivity in some of the more difficult reactions such as methanation and the Fischer–Tropsch syntheses may be due to the requirement for multinuclear centers to activate the substrate sufficiently.[1,4] Nevertheless, there is relatively little chemistry resulting in the generation of organic products that has been observed in stoi-

(1) Muettertles, E. L. *Angew. Chem., Int. Ed. Engl.* **1983**, *22*, 135 and references therein.

(2) See, for example: "Metal Clusters in Catalysis" In *Studies in Surface Science and Catalysis*; Gates, B. C., Guczi, L., Knozinger, H., Eds.; Elsevier: New York, 1986; Vol. 29.

(3) See, for example: (a) Dombek, B. D. *Organometallics* **1985**, *4*, 1707. (b) Beanan, L. R.; Keister, J. B. *Ibid.* **1985**, *4*, 1713.

(4) Anderson, R. B. *The Fischer–Topsch Synthesis*; Academic Press: Orlando, FL, 1984.

0002-7863/88/1510-5744$01.50/0